JAN 17 1947

ARR No. 3D16

NATIONAL ADVISORY COMMITTEE FOR AERONAUTICS

WARTIME REPORT

ORIGINALLY ISSUED

April 1943 as
Advance Restricted Report 3D16

AN INVESTIGATION OF AIRCRAFT HEATERS

XI - MEASURED AND PREDICTED PERFORMANCE OF A SLOTTED-FIN EXHAUST GAS AND AIR HEAT EXCHANGER

By L. M. K. Boelter, M. A. Miller,
W. H. Sharp, and E. H. Morrin
University of California

NACA

WASHINGTON

W-15

NATIONAL ADVISORY COMMITTEE FOR AERONAUTICS

ADVANCE RESTRICTED REPORT

AN INVESTIGATION OF AIRCRAFT HEATERS

XI - MEASURED AND PREDICTED PERFORMANCE OF A SLOTTED-FIN EXHAUST GAS AND AIR HEAT EXCHANGER

By L. M. K. Boelter, M. A. Miller,
W. H. Sharp, and E. H. Morrin

SUMMARY

Thermal and pressure drop performance data of a slotted-fin Stewart-Warner exhaust gas and ventilating air heat exchanger are presented. Measurements were made, using up to 7000 pounds per hour of exhaust gas and up to 5000 pounds per hour of ventilating air. The inlet exhaust gas temperature was maintained at about 1400° F; whereas that of the ventilating air was about 95° F.

Three different crossflow air shrouds were used in these tests. The effect of installing a "central core" in the exhaust gas side of the heater was determined. Isothermal and non-isothermal static pressure drop measurements were made on both the exhaust gas and ventilating air sides of the heater. Isothermal pressure drops across the inlet and outlet ducts of the air shrouds were measured. Temperatures of the heater surfaces at several points were also recorded.

Measured and predicted heat transfer rates and pressure drops are compared. The maximum measured rate of heat transfer was 216,000 Btu per hour. The maximum measured non-isothermal pressure drop on the ventilating air side, using a semi- or diagonal-crossflow air shroud was 16.5 inches of water; whereas that using a full crossflow shroud was 5.3 inches of water. The maximum measured pressure drop on the exhaust gas side of the heater was 9.8 inches of water before the central core was installed and 16.9 inches of water after the central core was in place. The maximum heater-surface temperature was 1120° F.

INTRODUCTION

The Stewart-Warner heater was tested on the large test stand in the Mechanical Engineering Laboratories of the University of California. (See fig. 1, and description of test stand in reference 1.)

These heaters are used in the exhaust gas streams of aircraft engines for cabin, wing, and tail-surface heating systems.

The following data were obtained:

1. Weight rates of exhaust gas and ventilating air through the two sides of the heat exchanger

2. Temperatures of exhaust gas and of ventilating air at entrance and exit of heat exchanger

3. Temperatures of the heater surfaces

4. Static pressure drop measurements on the exhaust gas and ventilating air sides of the heater and ducts, under both isothermal and non-isothermal flow conditions

5. Isothermal static pressure drop measurements across the inlet and outlet air-shroud ducts alone

The measurements were made with three different ventilating air shrouds and also with and without a "central core" installed in the exhaust gas side of the heater.

SYMBOLS

A area of heat transfer, ft^2

A_a cross-sectional area of one fin on the ventilating air side of the heater, ft^2

A_g cross-sectional area of one fin on the exhaust gas side of the heater, ft^2

$A_{spot\text{-}weld}$ cross-sectional area of spot welds, ft^2 (See appendix.)

A_{u_a} unfinned base area on the ventilating air side of the heater, ft^2

A_{u_g} unfinned base area on the exhaust gas side of the heater, ft^2

c_{p_a} heat capacity of air at constant pressure, Btu/lb °F

c_{p_g} heat capacity of exhaust gas at constant pressure, Btu/lb °F

D hydraulic diameter, ft

D_a hydraulic diameter on ventilating air side, ft

D_g hydraulic diameter on exhaust gas side, ft

f_c unit thermal convective conductance (average with length), Btu/hr ft^2 °F

f_{c_a} unit thermal convective conductance for the ventilating air (average with length), Btu/hr ft^2 °F

f_{c_g} unit thermal convective conductance for the exhaust gas (average with length), Btu/hr ft^2 °F

g gravitational force per unit of mass, lb/(lb sec^2/ft)

G weight rate per unit of area, lb/hr ft^2

G_a weight rate per unit of area for ventilating air, lb/hr ft^2

G_g weight rate per unit of area for exhaust gas, lb/hr ft^2

k thermal conductivity of fin material, Btu/hr ft^2 (°F/ft)

k_s thermal conductivity of Inconel heater shell, Btu/hr ft^2 (°F/ft)

L distance between static-pressure measuring stations and length of heat transfer surface, ft

L_a length of fins on ventilating air side of heater measured perpendicularly to the heater shell, ft

L_g length of fins on exhaust gas side of heater measured perpendicularly to the heater shell, ft

L_s thickness of heater shell, ft

n_a number of fins on ventilating air side

n_g number of fins on exhaust gas side

P heat transfer perimeter of one fin on either side of heater, ft

q_a measured rate of enthalpy change of ventilating air, Btu/hr

q_g measured rate of enthalpy change of exhaust gas, Btu/hr

R_{total} total thermal resistance including that through heater shell, $^{\circ}$F hr/Btu

t_a arithmetic average of temperatures measured by two thermocouples located on heater shell near ventilating air <u>inlet</u> (one thermocouple at exhaust gas inlet, the other at exhaust gas outlet), $^{\circ}$F

t_b arithmetic average of temperatures measured by two thermocouples located on heater shell near ventilating air <u>outlet</u> (one thermocouple at exhaust gas inlet, the other at exhaust gas outlet), $^{\circ}$F

t_c arithmetic average of temperatures measured by two thermocouples located on heater shell equidistant from ends (one thermocouple on top, the other on the bottom), $^{\circ}$F

T_a arithmetic average mixed-mean absolute temperature of either fluid $= \dfrac{T_1 + T_2}{2}$, in equation (11) only; otherwise arithmetic average mixed-mean absolute temperature of air $= \dfrac{T_{a_1} + T_{a_2}}{2} + 460$, $^{\circ}$R

T_g arithmetic average mixed-mean absolute temperature of exhaust gas $= \dfrac{T_{g_1} + T_{g_2}}{2} + 460$, $^{\circ}$R

T_1 mixed-mean absolute temperature of fluid at entrance section (point 1), $^{\circ}$R

T_2 mixed-mean absolute temperature of fluid at exit section (point 2), $^{\circ}$R

T_{iso} mixed-mean absolute temperature of fluid for isothermal pressure drop tests, °R

u_m mean velocity of fluid, ft/sec

U over-all unit thermal conductance, Btu/hr ft^2 °F

UA over-all thermal conductance, Btu/hr °F

$(UA)_{total}$ over-all thermal conductance including heater shell conductance, Btu/hr °F

W weight rate of fluid, lb/hr

W_a weight rate of air, lb/hr

W_g weight rate of exhaust gas, lb/hr

γ_1 weight density of fluid at entrance to heating section (point 1), lb/ft^3

ΔP non-isothermal pressure drop along heater, lb/ft^2

ΔP_a pressure drop along heater on ventilating air side, lb/ft^2

$\Delta P'_a$ pressure drop along heater on ventilating air side, inches H_2O

ΔP_g pressure drop along heater on exhaust gas side, lb/ft^2

$\Delta P'_g$ pressure drop along heater on exhaust gas side, inches H_2O

ΔP_{DUCT} isothermal pressure drop along inlet and outlet ducts of the air shroud, lb/ft^2

ΔP_{HTR} isothermal pressure drop along heater only, lb/ft^2

$\Delta P_{T_{iso}}$ isothermal pressure drop along heater and ducts at temperature T_{iso}, lb/ft^2

ζ_{iso} isothermal friction factor defined by $\frac{\Delta P}{\gamma} = \zeta_{iso} \frac{L}{D} \frac{u_m^2}{2g}$

Δt temperature difference, °F

Δt_{lm} logarithmic mean temperature difference, °F

ΔT_a difference between mixed-mean temperatures of ventilating air at sections defined by points 1 and 2 = $T_{a_2} - T_{a_1}$, $^{\circ}F$

ΔT_g difference between mixed-mean temperatures of exhaust gas at sections defined by points 1 and 2 = $T_{g_1} - T_{g_2}$, $^{\circ}F$

μ viscosity of fluid, lb sec/ft^2

T_{a_1} mixed-mean temperature of ventilating air at entrance section (point 1), $^{\circ}F$

T_{a_2} mixed-mean temperature of ventilating air at exit section (point 2), $^{\circ}F$

T_{g_1} mixed-mean temperature of exhaust gas at entrance section (point 1), $^{\circ}F$

T_{g_2} mixed-mean temperature of exhaust gas at exit section (point 2), $^{\circ}F$

Nu Nusselt number = $\dfrac{f_c D}{k}$

Pr Prandtl number = $\dfrac{3600\ \mu\ c_p\ g}{k}$

Re Reynolds number = $\dfrac{G\ D}{3600\ \mu\ g}$

Re_p Reynolds number = $\dfrac{G\ P}{3600\ \mu\ g}$

DESCRIPTION OF STEWART-WARNER SLOTTED-FIN HEATER AND TESTING PROCEDURE

The Stewart-Warner slotted-fin, exhaust gas and ventilating air heat exchanger is a crossflow-type heater. The slotted fins on the inner or exhaust gas side are placed longitudinally; whereas those on the outer or ventilating air side are placed circumferentially on the heater shell. There are 52 rows of fins on the air side of the heater and 80 rows on the exhaust gas side. Each row on the air side is cut at 1/4-inch intervals so that there are 69 fins per row. On the exhaust gas side each row is slotted at 3/4-inch intervals, yielding 19 fins per row. The fins are constructed of 0.045-inch copper and are spot-welded to a stainless steel shell. The fins on both sides of the heater are 3/4 inch in length measured perpendicularly to the shell.

The first air shroud tested with the Stewart-Warner heater was a diagonal- or semi-crossflow-type shroud obtained from the Ames Aeronautical Laboratory, Moffett Field, Calif. The inlet duct contained vanes which tended to direct the air over the heater at right angles. (See figs. 2 and 4.) Another air shroud (hereafter designated as UC-2) was constructed with dimensions equivalent to those of the Ames shroud, but with full crossflow characteristics. (See figs. 2 and 5.) A third air shroud (hereafter designated as UC-1) was constructed with full crossflow characteristics, but with a smaller clearance between the heater shell and the shroud.

In order to force the exhaust gas between the longitudinal slotted fins, a central core was installed on the gas side of the heater. (See figs. 2 and 6.)

The weight rates of exhaust gas and ventilating air were obtained by means of calibrated square-edge orifices.

The exhaust gas temperatures were measured at the inlet and the outlet of the heater by means of shielded traversing thermocouples.

A mixing device was used at the exit of the natural gas furnace to given an approximately uniform temperature distribution at the entrance to the heater. (The measured temperature distribution in degrees Fahrenheit was within ±3 percent of complete uniformity at the inlet end of the heater.)

No mixing device was used downstream from the heater on the exhaust gas side. The measured temperature distribution in degrees Fahrenheit was thus within ±3 percent of complete uniformity, which was reduced to $\pm 1\frac{1}{2}$ percent when the central core was installed because of the greater mixing encountered when the gas expanded into the outlet exhaust gas duct. (See reference 1 for a description of the test stand and its instrumentation.)

For all shrouds, the exhaust gas temperature traverses were made at points 15 inches upstream and 24 inches downstream from the ends of the heater.

Temperatures of the ventilating air before and after passage through the heater were determined from traverses made with unshielded thermocouples. Runs 22 to 51 were made without a mixing device in the ventilating air outlet duct. For these runs the temperature distribution was within ±9 percent of complete uniformity. For runs 52 to 122, a 3-inch diameter orifice was installed in the 5-inch diameter outlet air duct to cause better mixing of the fluid through its sudden expansion downstream from the orifice. The temperature distribution thus obtained was within ±2 percent of complete uniformity.

For the Ames air shroud, temperature traverses of the ventilating air were made at points 26 inches upstream and 50 inches downstream from the center line of the heater.

The heat losses to the surroundings were reduced to a negligible amount by wrapping the ducts with asbestos sheets.

Temperatures of the heater surfaces were measured at six points by means of thermocouples. One pair of thermocouples was located on the heater shell near the ventilating air inlet side (one thermocouple near the exhaust gas inlet, the other thermocouple near the exhaust gas outlet). The arithmetic average of these two temperatures is designated as t_a. A second pair of thermocouples was located near the ventilating air outlet side (one thermocouple near the exhaust gas inlet, the other near the exhaust gas outlet). The arithmetic average of these two temperatures is designated as t_b. The third pair of thermocouples was located on the heater shell equidistant from the ends (one thermocouple on top, the other on the bottom). The arithmetic average of these two temperatures is designated as t_c. (See fig. 2.)

Static pressure drop measurements were made across the ventilating air and exhaust gas sides of the heater. Two taps, 180° apart, were installed at each pressure-measuring station. For all shrouds, the pressure taps on the exhaust gas side were placed on the heater shell about $2\frac{1}{2}$ inches from the ends of the heater. For the Ames shroud, the pressure taps on the ventilating air side were placed about 12 inches upstream and downstream from the center line of the heater; whereas, for the UC-1 and UC-2 shrouds, the pressure taps on the ventilating air sides were placed in a 5-inch duct 30 inches upstream and downstream from the center line of the heater.

Isothermal pressure drops along the inlet and outlet air-shroud ducts were measured by detaching these ducts from the shroud and placing them together to obtain the total pressure drop across the two ducts. The air shrouds UC-1 and UC-2 utilized the same inlet and outlet ducts. When the inlet and outlet ducts used on the Ames semi-crossflow shroud were placed together, a very sharply curved path for the air was formed, and the measured pressure drop for the ducts placed in this manner was as large as the measured isothermal value across both the ducts and the heater when used in the normal arrangement. A truer value of the pressure drops through the ducts alone was obtained by placing a "spacer" equivalent to the width of the air shroud between the inlet and outlet ducts so that the ducts were in the same relative position for these tests and for those tests using both the air shroud and the heater. The pressure drop in this "spacer" was negligible (2 percent) compared with that across the converging and diverging, outlet and inlet air ducts.

CALCULATIONS

Heat Transfer

The thermal output of the heater was determined by the enthalpy changes of the ventilating air:

$$q_a = W_a\, c_{p_a}(\tau_{a_2} - \tau_{a_1}) \tag{1}$$

in which c_{p_a} was evaluated at the arithmetic average ventilating air temperature as a good approximation. A plot of q_a against w_a at constant values of exhaust gas rate W_g and inlet temperature τ_{g_1} is shown in figures 7 to 12.

On the exhaust gas side of the heater:

$$q_g = W_g\, c_{p_g}(\tau_{g_1} - \tau_{g_2}) \tag{2}$$

where c_{p_g} is evaluated for air at the temperature at the arithmetic average exhaust gas temperature.

The over-all thermal conductance UA was evaluated from the expression:

$$q_a = (UA)\Delta t_{lm} \tag{3}$$

The value of Δt_{lm} for cross flow is chosen as that for counterflow and then multiplied by a correction factor. (See reference 2.) Inasmuch as this correction factor was always within 1 percent of unity, the Δt_{lm} used in these calculations was taken to be that for counterflow of the fluids.

A plot of UA as a function of the ventilating air rate W_a at constant values of the exhaust gas rate W_g is shown in figures 13 to 18.

The thermal output of the heater may be predicted when used at other values of Δt_{lm} than those used in these tests by determining UA at the corresponding fluid weight rates from figures 13 to 18 and using these magnitudes in equation (3) with the new values of Δt_{lm}.

Predictions of the magnitudes of the over-all thermal conductance UA were attempted. The expression (reference 3, equation (28))

$$UA = \frac{1}{\left(\frac{1}{f_c A}\right)_{e_a} + \left(\frac{1}{f_c A}\right)_{e_g}} \tag{4}$$

where $\left(\frac{1}{f_c A}\right)_{e_a}$ and $\left(\frac{1}{f_c A}\right)_{e_g}$ are the effective thermal resistances on the air and exhaust gas sides of the heater, respectively, was used.

The effective thermal conductances, $(f_c A)_{e_a}$ and $(f_c A)_{e_g}$, are obtained from equations (see reference 3 for the derivation of equations (5) to (8)).

$$(f_c A)_{e_a} = n_a \left[\sqrt{f_{c_a} P k A_s} \tanh L_a \sqrt{\frac{f_{c_a} P}{k A_s}}\right] + f_{c_a} A_{u_a} \tag{5}$$

and

$$(f_c A)_g = n_g \left[\sqrt{f_{c_g} P k A_g} \tanh L_g \sqrt{\frac{f_{c_g} P}{k A_g}} \right] + f_{c_g} A_{u_g} \quad (6)$$

where

A cross-sectional area of one fin

k thermal conductivity of fin material evaluated at an average temperature

P heat transfer perimeter of one fin

L length of one fin measured perpendicularly to heater shell

n_a total number of fins on air side of heater

n_g total number of fins on exhaust gas side

f_c unit thermal conductance along fins and along unfinned area A_u of heater

For the exhaust gas side f_{c_g} is evaluated from the equation

$$f_{c_g} = 5.56 \times 10^{-4} \; T_g^{0.296} \frac{G_g^{0.8}}{D_g^{0.2}} \quad (7)$$

where

T_g arithmetic average absolute temperature

G_g exhaust gas weight rate per unit cross-sectional area

D_g hydraulic diameter of space (channel) between rows of fins on exhaust gas side

Because the slots on the exhaust gas side were narrow, their effect on the fluid flow and unit thermal conductance was neglected and f_{c_g} was calculated by means of equation (7), which is based upon flow in pipes and channels where the characteristic dimension is the hydraulic diameter.

On the air side, the circumferential fins were slotted at 1/4-inch intervals. The Reynolds number using the perimeter P of the fin as the significant dimension $Re_P = \frac{G P}{3600 \mu g}$ varies from 10,000 to 25,000, so that the boundary layer over each fin may be laminar* for a considerable length along the fin. The f_{c_a} for the laminar regime is then evaluated from equation (6) of reference 5:

$$f_{c_a} = 0.112\, T^{0.5}\left(\frac{u_m\,\gamma}{L}\right)^{0.5} \qquad (8)$$

but since $3600\, u_m\, \gamma = G$

$$f_{c_a} = 1.87 \times 10^{-3}\, T^{0.5}\left(\frac{G}{L}\right)^{0.5} \qquad (9)$$

For this heater, L is 1/4 inch on the ventilating air side. The magnitude of the unit thermal conductance f_{c_a} along the unfinned base areas between the rows of fins is probably not the same as that along the fins.

If the f_{c_a} along the unfinned base areas is calculated on the basis of the hydraulic diameter of the channel between the rows of fins, its value is found to be about one-half that of f_{c_a} calculated for laminar flow over the fins. The heat transfer along this unfinned area is thus about 10 percent of the total when the f_{c_a} based on hydraulic diameter is used and is about 17 percent of the total when the f_{c_a} based on laminar flow over the fins is used. The heat transfer from the unfinned area therefore need not be accurately known. The actual value of f_{c_a} is probably between the two mentioned.

Pressure Drop

Measurements of the static pressure drops across the air and exhaust gas sides of the heat were made for isothermal $\Delta P_{T_{iso}}$ and non-isothermal conditions ΔP. Also, pressure drops were determined for the air inlet and outlet ducts alone under isothermal conditions. The measured pressure drops on the exhaust gas side did not include the losses in the ducting; so $\Delta P_{T_{iso}} = \Delta P_{HTR}$ where ΔP_{HTR} is the pressure drop along the heater alone.

*The results of R. H. Norris and W. A. Spofford (reference 4) indicate that the boundary layer over groups of flat plates and cylindrical fins is laminar for $Re_p < 20{,}000$. Equations (8) and (9) are equivalent to equation (1) of reference 4.

For the exhaust gas side the expression

$$\frac{\Delta P_{HTR}}{\gamma} = \zeta_{iso} \frac{L}{D} \frac{u_m^2}{2g}$$

was used to determine the dimensionless modulus,

$$\left(\zeta_{iso} \frac{L}{D}\right) = \frac{2g}{u_m^2} \left(\frac{\Delta P_{HTR}}{\gamma}\right)$$

or

$$\left(\zeta_{iso} \frac{L}{D}\right) = 2 \, g \, \gamma \frac{\Delta P_{HTR}}{\left(\frac{G_g}{3600}\right)^2} \tag{10}$$

For the ventilating air side,

$$\Delta P_{HTR} = \Delta P_{T_{iso}} - \Delta P_{DUCT}$$

thus

$$\left(\zeta_{iso} \frac{L}{D}\right) = 2 \, g \, \gamma \frac{\Delta P_{HTR}}{\left(\frac{G_a}{3600}\right)^2} \tag{10a}$$

The pressure drops through the ducts on the air side for the three air shrouds and the modulus $\left(\zeta_{iso} \frac{L}{D}\right)$ for the exhaust gas and air sides of the heater are tabulated in tables VII and VIII.

The non-isothermal pressure drop of either fluid through the heat exchanger was predicted from isothermal measurements by means of equation (6) of reference 1.

$$\Delta P = \Delta P_{T_{iso}} \left(\frac{T_a}{T_{iso}}\right)^{1.13} + \left(\frac{G}{3600}\right)^2 \frac{1}{\gamma_1 g} \left(\frac{T_2}{T_1} - 1\right) \tag{11}$$

where

$\Delta P_{T_{iso}}$ total measured isothermal pressure drop due to friction at temperature T_{iso}

T_1 and T_2 mixed-mean absolute temperatures of fluid at inlet and exit of heater, respectively

T_a arithmetic average of T_1 and T_2.

G fluid flow per unit cross-sectional area

γ_1 unit weight of fluid at inlet to heater evaluated at temperature T_1

A comparison of measured and predicted non-isothermal pressure drops through both sides of the heater is presented in tables IX and X and is shown graphically in figures 19 to 23.

Heat transfer and pressure drop data for the Stewart-Warner heater are presented in tables I and II for the tests using the Ames air shroud, in tables III and IV for those using the UC-1 air shroud, and in tables V and VI for those using the UC-2 air shroud.

DISCUSSION OF RESULTS ON THE STEWART-WARNER HEATER*

The enthalpy change of the ventilating air was used to determine the thermal output of the heater, for these measurements were more accurate than those on the exhaust gas side of the heater. The arithmetic average heat balance ratio q_g/q_a of all the tests was 0.78. It can be shown that a 1-percent error in the determination of either exhaust gas temperature $T_g \approx 1400°$ F may cause a 20-percent error in the temperature change of the exhaust gas. The low heat balance ratios obtained in these tests may be due to this error in measurement; they also may be due to incomplete combustion of the exhaust gases.

Three air shrouds were used in these tests.

1. Semi- or diagonal-crossflow shroud (designated as Ames air shroud). Clearance between heater shell and air shroud is $1\frac{5}{16}$ inches.

---

*See also report by R. A. Kepner and A. R. Collins (reference 6) on results of tests performed on similar heaters in the Heater Laboratory of the Stewart-Warner Co., Chicago.

2. Full crossflow shroud (designated as UC-2 air shroud). Clearance between heater shell and air shroud is $1\frac{5}{16}$ inches (same as Ames air shroud).

3. Full crossflow shroud (designated as UC-1 air shroud). Clearance between heater shell and air shroud is 1 inch.

Thus a comparison of the results obtained when using the Ames semi-crossflow and the UC-2 full crossflow air shrouds will reveal the effect, on the heat transfer rate and the pressure drop, of the direction or manner in which the ventilating air is conducted across the heater, since all physical dimensions were identical for these two air shrouds. A comparison of the results obtained when using the air shrouds UC-1 and UC-2 will reveal the effect, on the pressure drop and the rate of heat transfer, of decreasing the cross-sectional area on the ventilating air side of the heater.

During the preliminary tests of the heater, it was discovered that the rate of heat transfer was inappreciably affected by an increase of the exhaust gas rate W_g from 6000 to 7500 pounds per hour. (See figure 7.) This was an indication that the exhaust gases were passing through the center of the heater and not through the channels between the rows of fins. In order to ameliorate this effect, a central core was installed in the exhaust gas side of the heater which forced the gases to flow through the channels between the rows of fins. The measured rates of heat transfer were thus increased and varied appreciably when the exhaust gas weight rate W_g was increased from 6100 to 7100 pounds per hour. (See fig. 8.)

A comparison of figures 13, 15, and 17 reveals that, for the heater <u>without the central core</u> in the exhaust gas side, the over-all thermal conductance UA at W_a = 4000 pounds per hour and W_g = 6900 pounds per hour was about 137 Btu/hr °F using the Ames air shroud, 142 Btu/hr °F using the UC-1 air shroud, and 128 Btu/hr °F using the UC-2 air shroud.

Since the cross-sectional areas and other dimensions were the same for the Ames semi-crossflow shroud and the UC-2 full-crossflow shroud, the increase of 9 Btu/hr °F when using the Ames shroud must have been due to the greater air turbulence, since the air probably flowed diagonally across the rows of slotted fins and not directly between the fins as with the UC-2 shroud.

The increase of 14 Btu/hr °F when using the UC-1 shroud over the result obtained when using the UC-2 shroud was due to the decreased cross-sectional area of the former (1-in. clearance between heater shell and shroud as against $1\frac{5}{16}$-in. clearance), since all other dimensions and physical characteristics were identical for the two UC air shrouds.

The greater over-all thermal conductance obtained in the runs using the UC-1 air shroud as compared to the runs using the Ames air shroud was due to the decreased cross-sectional area of the former, a factor which outweighed the turbulence-forming characteristics of the diagonal- or semi-crossflow Ames shroud. This greater heat transfer rate when using the smaller, but full-crossflow, UC-1 shroud was obtained with a much smaller static pressure drop.

The measured isothermal pressure drop along the air side of the heater (inlet and outlet air-duct losses subtracted) at an air rate of 3000 pounds per hour was 12.4 pounds per square foot (2.40 in. of water) using the Ames semi-crossflow shroud, 5.45 pounds per square foot (1.05 in. of water) for the UC-2 shroud, and 8.45 pounds per square foot (1.63 in. of water) for the UC-1 air shroud.

Thus more than double the pressure drop is encountered when the ventilating air is not caused to flow directly along the space between the fins, but is allowed to flow somewhat diagonally across the rows of fins (cf. pressure drops using Ames and UC-2 air shrouds (figs. 19 and 21).

The pressure drop was decreased to about 70 percent of the measured value for the Ames shroud by using the UC-1 shroud, which was fully crossflow but had an even smaller cross-sectional area. (See figs. 19 and 20.)

It can be said, therefore, that the increase of the thermal conductance due to the greater turbulence along the slotted fins when using the diagonal crossflow shroud is more than counterbalanced when using the full crossflow shroud by decreasing the air side clearance from $1\frac{5}{16}$ inches to 1 inch. The isothermal and non-isothermal pressure drops for the latter clearance are only about 70 percent of the value for the diagonal crossflow shroud.

This large increased pressure drop for the semi-crossflow shroud would not be found when this shroud is used on other types of heaters, such as pin-fin heaters; although it would be experienced when it is used on all heat exchangers with circumferential, continuous or semi-continuous (slotted) fins. Because the air is deflected to flow over the heater, the pressure drop in the inlet and outlet ducts is about 40 percent of the total pressure drop with the heater installed. This pressure drop through the ducts of the Ames shroud was as much as the total pressure drop along the ducts and across the heater when the UC-2 shroud was used. The pressure drop through the inlet and outlet ducts was, with the heater installed, about 20 percent of the total drop using the UC-2 shroud and about 14 percent using the UC-1 shroud.

When the central core (diam. $2\frac{3}{8}$ in.) was placed in the exhaust gas side of the heater, the net cross-sectional area was decreased by 15 percent. Thus the over-all thermal conductance, with the central core installed (see figs. 14, 16, and 18), for W_a = 4000 pounds per hour and W_g = 6900 pounds per hour was about 153 Btu/hr °F for the runs with the semi-crossflow shroud, 157 Btu/hr °F using the UC-1 shroud, and 140 Btu/hr °F using the UC-2 shroud. These results are about 9 to 12 percent higher than those obtained without the central core installed, owing to the increased value of $G = \frac{W}{\text{area}}$ in the space between the fins on the exhaust gas side of the heater. This result was brought about both by decreasing the net cross-sectional area of flow and by forcing the gas to flow through the spaces between the fins rather than through the open central space.

The increase in UA due only to the decrease in the net cross-sectional area (increased G) was calculated to be 5 to 6 percent; thus the remainder of the 9 to 12 percent increase in UA reported above must have been due to forcing the exhaust gases to flow through the spaces between the fins.

The increase in UA by use of the central core would have been much greater at higher exhaust gas rates (say 7500 lb/hr) than the increase reported above for W_g = 6900 pounds per hour. An inspection of figure 13 reveals that when the central core was not used UA did not change appreciably when W_g was increased from 6000 to 7500 pounds per hour, but the use of the central core partially remedied this condition. (See fig. 14.*)

The use of the central core doubled the static pressure drop on the exhaust gas side of the heater. At an exhaust gas rate of 6000 pounds per hour, the <u>isothermal</u> pressure drop increased from about 10 pounds per square foot (1.92 in. of water) to about 20 pounds per square foot (3.84 in. of water). The increase in the isothermal pressure drop due merely to the decreased net cross-sectional area (increased G) would have been only about 40 percent or 4 pounds per square foot (0.77 in. of water). Thus the remainder of the 10 pounds per square foot pressure drop increase resulting from use of the central core was due to the increased flow in the channels or spaces between the rows of slotted fins. The measured and predicted <u>non-isothermal</u> pressure drops were also about twice as large when the central core was used. (Cf. figs. 22 and 23.)

The arithmetic average of all the slopes of the ΔP against W curves (figs. 19 to 23) is 1.79. This value of the exponent is to be expected, for the isothermal <u>frictional</u> pressure drop is proportional to $\zeta_{iso} W^2$ and because ζ_{iso}, the isothermal friction factor, is proportional to $W^{-0.2}$ ($\zeta_{iso} \propto Re^{-0.2}$) for the turbulent regime, thus the static pressure drop ΔP is proportional to $W^{2.0-0.2}$ or $W^{1.80}$. However, the pressure drop on the air side of the heater using the semi-crossflow shroud is due not entirely to friction but partly to eddy and wake-formation losses.

An inspection of the pressure drop plots reveals that, for the air side of the heater, the slope of the non-isothermal pressure drop curve is less than that of the isothermal curve. It can be shown that, for the ventilating-air side the <u>slope</u> of the non-isothermal curve must be <u>less</u> than the isothermal one, because the former is a <u>higher</u> value (the temperature of the air is higher) and must coincide with the isothermal value at

---

*The effect due to the use of the central core is not shown as clearly by the results from tests using the UC-1 and UC-2 air shrouds; since the highest values of exhaust gas rate, where the effect would have been most noticeable were not attainable, owing to the additional resistance caused by the presence of the core.

an infinite air rate, for which condition the temperature rise of the air would be zero ($T_{iso} = T_{a_1} = T_{a_2}$, i.e., isothermal). (See figs. 19, 20, and 21.)

For the exhaust gas side, the non-isothermal curve should have a greater slope than the isothermal curve because the exhaust gas is cooled. The last term in equation (11) is negative for the case of a fluid being cooled and is less negative at high fluid rates, for the change in fluid temperature is then less. Also the first term on the right side of equation (11) is slightly higher for high fluid rates, since the T_a is greater (fluid does not cool as much at high fluid rates for the same heat transfer rate as at low fluid rates). Thus the combination of a term which increases with fluid rate and another term which becomes less negative at high fluid rates yields a sum which increases with the fluid rate, and therefore the slope of the non-isothermal pressure drop curve would be greater than that of the isothermal curve. (See figs. 22 and 23.)

The calculated values of $\left(\zeta_{iso} \frac{L}{D}\right)$ do not indicate any specific correlation of the results obtained with the different air shrouds and on both sides of the heater. (See tables VII and VIII.)

On the exhaust gas side, the value of ζ_{iso} could be predicted within 8 to 30 percent by means of the friction factor against Reynolds number relation for commercial pipes, evaluating Re for the channel or space between the fins. (See reference 3, fig. 7.)

It is very difficult to predict the magnitude of ζ_{iso} for the flow along the narrow fins on the ventilating air side of the heater.

The agreement between the measured and predicted non-isothermal pressure drops along the exhaust gas side of the heater is very good. The corresponding agreement for the air side is not so good since the pressure drop over the narrow fins on the air side is due, to a great extent, to causes other than friction (i.e., eddy and wake-formation losses) especially for the Ames semi-crossflow shroud. The value of $\Delta P_{T_{iso}}$ which is to be substituted in equation (11) to obtain the predicted frictional non-isothermal pressure drop should be that due to friction alone.

The average heater surface temperature on the side of the heater where the ventilating air entered was about 750° F; whereas that near the ventilating air outlet was about 1000° F. The temperature of the heater-shell surface at a point intermediate between the entrance and exit air openings was lower in most runs than that at the air entrance or exit. This result is questionable, for the lowest temperature should be found near the point where the cool air impinges on the heater (i.e., near the ventilating air inlet). The thermocouple lead-in wires were conducted through the ventilating air stream and although they were thermally insulated some error in the temperature measurement was to be expected because of the "cooling effect" of the air on the lead-in wires.

The predicted magnitudes of UA were about 80 percent above those derived from laboratory measurements. This discrepancy was probably due to the following two reasons:

1. The value of the weight rate per unit area G of either fluid calculated from the total weight rate and the net cross-sectional area probably did not obtain in the restricted channels between the rows of fins. The actual fluid velocities along the fins or channels were smaller than those in the center of the fluid passages.

2. The external and internal fins were not placed in intimate contact with the heater shell. Only an area of about one-half the total cross-sectional area of the fins was welded to the heater shell by means of small spot welds. The spot welds which were in direct contact with the base metal were placed on the average at approximately 3/4-inch intervals along the base of the fins. The area which was not spot-welded could have been insulated from the base by a small gas film or scale. (See appendix.)

This condition may cause failure owing to excessive local temperatures on the gas side when used in an actual aircraft installation.

If the heater were constructed without fins but operated so that the same values of f_c were obtained as were found along the fins, the magnitude of UA at W_a = 5000 pounds per hour and W_g = 4490 pounds per hour would be 47 Btu/hr °F. The measured UA for the finned heater (using UC-1 shroud and central core) was 144 Btu/hr °F;

whereas the predicted value was 262 Btu/hr °F. Hence the magnitude of UA was increased 97 Btu/hr °F by the addition of the fins, but an increase of about 215 Btu/hr °F could be obtained by a more perfect fusing of the fins to the heater shell.

The correction to the equations for evaluating the unit thermal conductance f_c due to the variation of f_c near the inlet to a pipe, channel, or space between adjacent fins (see reference 7) is negligible in the computation of the f_c for this heater. On the exhaust gas side the ratio of the hydraulic diameter of the channel or space between the slotted fins to the length of the channel (i.e., D/L) is 0.023; and, since the correction to equation (7) for this "D/L effect" is the multiplier $1 + 1.1\ D/L$, the corrected f_c would be only about 3 percent greater than that computed by means of equation (7) as written above.

On the ventilating air side the fins are so narrow (1/4 in.) that the boundary layers along these fins are probably laminar, and equation (9) applies without the correction factor mentioned.

CONCLUSIONS

1. The rate of heat transfer of the Stewart-Warner slotted-fin heater utilizing three different air shrouds was nearly the same for each (about a 10 percent difference between the semi- and the full-crossflow air shrouds).

2. The static pressure drops through the air side of the heater were greatly affected by use of the three air shrouds. The semi-crossflow shroud caused twice the pressure drop measured along the similar but full-crossflow shroud. The pressure drop was greater for the semi-crossflow shroud because of the pressure losses in the angular inlet and outlet ducts and also because the air was not completely deflected so that it flowed over the heater at right angles (i.e., between the rows of fins) but was allowed to flow somewhat diagonally across the rows of fins.

3. The thermal effectiveness of the copper-slotted fins used on this heater was considerably reduced by two

factors. First, the fluids did not flow in the spaces between the fins but, for the most part, flowed through the open parts of the exhaust gas and ventilating air passages. Secondly, the thermal resistance to heat transfer was greatly increased, owing to the limited contact area between the slotted fins and the heater shell. It would be advantageous to use a smaller number of more perfectly attached fins and thus obtain equivalent heat transfer rates but with considerably less pressure drop as well as effect a great saving in the weight of the finned heater. There also would be less danger of overheating some metal surfaces, such as the tips of the fins on the exhaust gas side, for the rate of heat transfer through a well-attached fin would be greater and its temperature would be correspondingly lower.

4. An attempt was made to force the exhaust gas to flow in the space between the fins instead of through the open central passage by installing a "central core" in this side of the heater. Without the use of this central core a considerable variation of high mangitudes of exhaust gas weight rates did not cause an appreciable change in the rate of heat transfer. The use of the central core, however, forced the exhaust gas to flow along the slotted fins and, together with the increase in exhaust gas rate per unit of cross-sectional area, caused the heat transfer rate to increase. The static pressure drop, however, was increased at a greater rate.

University of California,
Berkeley, Calif.

APPENDIX

The following method was used to predict the additional thermal resistance through the heater, owing to the imperfect contact between the slotted fins and the heater shell.

This additional thermal resistance consisted of three parts:

1. Thermal resistance from base of copper fins on exhaust gas side to point of spot weld

2. Thermal resistance through Inconel heater shell at point of spot weld

3. Thermal resistance from spot weld to base of copper fins on ventilating air side of heater

By means of a thermal flux plot (reference 8) the magnitudes of the first and third above-mentioned resistances were estimated to be 0.38×10^{-3} °F hr/Btu.

The second thermal resistance (through the spot weld in the Inconel shell) was evaluated from the expression

$$\frac{q}{\Delta t} = \frac{k_s\, A_{spot\text{-}weld}}{L_s} = \frac{1}{\text{resistance}}$$

The total area $A_{spot\text{-}weld}$, which was spot-welded (assuming one spot weld of 3/16-in. diam. per 3/4 in. measured along the fin base) was 0.153 square foot, the thermal conductivity k_s of Inconel was taken to be 15 Btu/hr ft² (°F/ft), and the thickness L_s of Inconel shell was 0.047 inch. Thus

$$\text{Resistance} = \frac{L_s}{k_s\, A_{spot\text{-}weld}} = \frac{0.047/12}{15 \times 0.153} = 1.70 \times 10^{-3}\ \frac{°F\ hr}{Btu}$$

The sum of the three thermal rosistance was then $(1.70 + 0.38)\ 10^{-3} = 2.08 \times 10^{-3}$ °F hr/Btu = R_{total}. The over-all thermal conductance UA was then obtained from

$$\left(\frac{1}{UA}\right)_{total} = \left(\frac{1}{f_cA}\right)_{e_a} + \left(\frac{1}{f_cA}\right)_{e_g} + R_{total}$$

but $\left(\frac{1}{f_cA}\right)_{e_a} + \left(\frac{1}{f_cA}\right)_{e_g}$ was the reciprocal of the over-all conductance UA previously computed, which neglected the additional resistances through the base of the fins and the heater shell. As mentioned under Discussion, the magnitude of UA at $W_a = 5000$ pounds per hour and $W_g = 4490$ pounds per hour was calculated to be 262 Btu/hr °F. Thus,

$$\left(\frac{1}{f_cA}\right)_{e_a} + \left(\frac{1}{f_cA}\right)_{e_g} = \frac{1}{UA} = \frac{1}{262} = 3.82 \times 10^{-3}\ °F\ hr/Btu$$

Therefore,

$$\left(\frac{1}{UA}\right)_{total} = (3.82 + 2.08)\ 10^{-3} = 5.90 \times 10^{-3}\ {}^{o}F\ hr/Btu$$

or

$$(UA)_{total} = 170\ Btu/hr\ {}^{o}F$$

The magnitude of UA for this heater derived from laboratory measurements was 144 Btu/hr ^{o}F.

At a lower air rate W_a = 2000 lb/hr, the predicted $(UA)_{total}$ was 148 Btu/hr ^{o}F by the method above, and the value derived from laboratory data was 116 Btu/hr ^{o}F.

Although the method indicated reveals that the resistance of the shell at the spot weld is one of the determinative resistances, it cannot be used for prediction of the characteristics of this heater. This is due to the fact that the assumptions with respect to the dimensions and the distribution of the spot welds were obtained by examination of two or three rows of fins on the inside and outside of the heater. Also, it was assumed that the heater shell and fins were in contact only at the spot welds.

These assumptions cannot be generalized, and hence the method is of limited utility for prediction of the thermal characteristics of this heater or others of a similar type. Exact knowledge of the dimensions and the number of the spot welds is necessary for accurate prediction, but that can be obtained only by destroying the heater.

Even if it were possible to obtain the necessary data for prediction of the resistance of the spot-welded shell, calculations of the thermal output would still be impeded by a lack of knowledge of the true weight rate per unit of cross-sectional area G of the ventilating air or exhaust gas along the spaces (or channels) between the rows of fins.

The authors wish to express appreciation to the following persons who helped obtain experimental data or prepare this report: Messrs. S. L. Scordelus, D. R. Ferguson, M. E. McLaughlin, G. T. Rowe, A. G. Guibert, and H. G. Dennison.

REFERENCES

1. Boelter, L. M. K., Miller, M. A., Sharp, W. H., Morrin, E. H., Iversen, H. W., and Mason, W. E.: An Investigation of Aircraft Heaters. IX - Measured and Predicted Performance of Two Exhaust Gas-Air Heat Exchangers and an Apparatus for Evaluating Exhaust Gas-Air Heat Exchangers. NACA ARR, March 1943.

2. McAdams, W. H.: Heat Transmission. McGraw-Hill Book Co., Inc., 2d ed., 1943, p. 147.

3. Martinelli, R. C., Weinberg, E. B., Morrin, E. H., and Boelter, L. M. K.: An Investigation of Aircraft Heaters. IV - Measured and Predicted Performance of Longitudinally Finned Tubes. NACA ARR, Oct. 1942.

4. Norris, R. H., and Spofford, W. A.: High-Performance Fins for Heat Transfer. Trans., A.S.M.E., vol. 64, no. 5, July 1942, pp. 489-496.

5. Martinelli, R. C., Guibert, A. G., Morrin, E. H., and Boelter, L. M. K.: An Investigation of Aircraft Heaters. VIII - A Simplified Method for the Calculation of the Unit Thermal Conductance over Wings. NACA ARR, March 1943.

6. Kepner, R. A., and Collins, A. R.: Performance Characteristics of Experimental Cross-Flow Exhaust-Gas Heat Exchangers. Stewart-Warner Corp., Chicago, Ill. Aug. 25, 1942.

7. Boelter, L. M. K., Dennison, P. G., Guibert, A. G., and Morrin, E. H.: An Investigation of Aircraft Heaters. X - Measured and Predicted Performance of a Fluted-Type Exhaust Gas and Air Heat Exchanger. NACA ARR, March 1943.

8. Boelter, L. M. K., Cherry, V. H., and Johnson, H. A.: Supplementary Heat Transfer Notes. Univ. of Calif. Press, Berkeley, Calif., 3d ed., 1942, p.IV-30.

TABLE I.– STEWART – WARNER #1 SLOTTED-FIN TYPE HEATER

AMES AIR – SHROUD ——— CENTRAL CORE NOT IN GAS SIDE

Run No.	AIR SIDE T_{a_1} °F	T_{a_2} °F	ΔT_a °F	W_a lbs/hr	ΔP_a Inches H_2O	q_a KBtu/hr	EXHAUST – GAS SIDE T_{g_1} °F	T_{g_2} °F	ΔT_g °F	W_g lbs/hr	ΔP_g Inches H_2O	q_g KBtu/hr	$\frac{q_g}{q_a}$	HEATER TEMPS. t_a °F	t_b °F	t_c °F	OVERALL PERFORMANCE Δt_{lm} °F	(UA) $\frac{Btu}{hr\,°F}$
22	102	303	201	2560	4.08	125	1415	1325	90	4230	3.10	105	0.84	TEMPERATURES NOT MEASURED			1170	107
23	100	263	163	3510	6.97	138	1437	1325	112	4280	3.15	132	0.96				1200	115
24	95	239	144	4190	9.60	146	1420	1312	108	4280	3.15	127	0.87				1200	122
25	97	225	128	4900	12.6	152	1437	1303	134	4280	3.15	158	1.04				1205	126
26	95	212	117	5650	15.9	160	1424	1308	116	4280	3.10	137	0.86				1210	132
27	96	228	132	5650	16.0	180	1419	1338	81	5965	6.20	133	0.74				1220	147
28	97	248	151	4920	13.1	180	1455	1356	99	5965	6.25	163	0.90				1230	146
29	97	255	158	4180	10.1	160	1446	1356	90	5965	6.25	148	0.92				1225	131
30	97	282	185	3510	6.57	157	1464	1373	91	5915	6.30	148	0.94				1225	128
31	97	322	225	2600	4.49	141	1428	1377	51	5915	6.40	83.0	0.59				1195	118
32	110	333	223	2620	4.85	141	1415	1368	47	7010	8.80	90.5	0.64				1170	120
33	113	298	185	3490	7.05	156	1433	1381	52	7020	8.80	100	0.64				1200	130
34	104	272	168	4230	10.6	172	1411	1343	68	7010	8.65	131	0.76				1190	144
35	108	254	146	4900	13.2	173	1407	1343	64	7020	8.70	124	0.72				1195	145
36	108	245	137	5700	16.5	189	1411	1343	68	6950	8.60	130	0.69				1200	158

NACA

(CONTINUED)

TABLE I.- STEWART — WARNER #1 SLOTTED-FIN TYPE HEATER

AMES AIR — SHROUD —— CENTRAL CORE NOT IN GAS SIDE

	AIR SIDE						EXHAUST — GAS SIDE							HEATER TEMPS.			OVERALL PERFORMANCE	
Run No.	T_{a_1} °F	T_{a_2} °F	ΔT_a °F	W_a $\frac{lbs}{hr}$	$\Delta P_a'$ Inches H_2O	q_a $\frac{KBtu}{hr}$	T_{g_1} °F	T_{g_2} °F	ΔT_g °F	W_g $\frac{lbs}{hr}$	$\Delta P_g'$ Inches H_2O	q_g $\frac{KBtu}{hr}$	$\frac{q_g}{q_a}$	t_a °F	t_b °F	t_c °F	Δt_{lm} °F	(UA) $\frac{Btu}{hr\,°F}$
37	104	242	138	5600	15.8	187	1398	1299	99	7530	9.30	205	1.10		TEMPERATURES		1175	159
38	104	254	150	4980	13.2	181	1403	1291	112	7530	9.35	232	1.28		NOT		1170	155
39	104	266	162	410	9.75	161	1390	1295	95	7530	9.50	197	1.22		MEASURED		1160	139
40	104	282	178	3460	7.40	149	1394	1308	86	7590	9.50	179	1.20				1155	129
41	105	335	230	2480	4.31	138	1394	1316	78	7590	9.70	163	1.18				1130	122
44	92	211	119	5650	15.3	162	1433	1304	129	4330	3.40	154	0.95				1210	134
45	90	228	138	5550	16.4	185	1428	1360	68	6060	6.70	114	0.62				1230	150
46	90	223	133	5580	15.8	179	1403	1321	81	6970	8.80	155	0.87				1205	148
47	89	225	136	5640	15.7	185	1420	1338	82	7580	9.80	171	0.92				1220	152

TABLE II.- STEWART - WARNER #1 SLOTTED-FIN TYPE HEATER

AMES AIR - SHROUD —— CENTRAL CORE IN GAS SIDE

	AIR SIDE						EXHAUST - GAS SIDE							HEATER TEMPS.			OVERALL PERFORMANCE	
Run No.	T_{a_1} °F	T_{a_2} °F	ΔT_a °F	W_a lbs/hr	$\Delta P_a'$ Inches H_2O	q_a KBtu/hr	T_{g_1} °F	T_{g_2} °F	ΔT_g °F	W_g lbs/hr	$\Delta P_g'$ Inches H_2O	q_g KBtu/hr	$\frac{q_g}{q_a}$	t_a °F	t_b °F	t_c °F	Δt_{lm} °F	(UA) Btu/hr°F
48D	98	252	154	5800	15.4	216	1437	1330	107	6880	16.0	203	0.94		TEMPERATURES NOT MEASURED		1215	178
49D	98	258	160	4950	13.0	192	1442	1373	69	6880	16.1	130	0.68				1230	156
50D	98	289	191	4220	10.2	195	1428	1373	55	6880	16.1	104	0.53				1205	162
51D	98	320	222	3020	5.88	162	1428	1381	47	6920	16.3	89.4	0.56				1200	135
52D	89	265	176	4600	5.95	196	1424	1364	60	7110	16.8	117	0.60				1210	162
53D	88	293	205	3770	4.70	187	1434	1390	43	7120	16.9	84.0	0.45				1220	153
54D	87	327	240	2830	3.14	164	1424	1368	56	6870	17.1	106	0.65				1240	132
55D	83	249	166	4600	5.85	185	1424	1334	90	6160	13.8	153	0.83				1215	152
56D	83	277	194	3790	4.57	178	1428	1347	81	6090	13.8	136	0.76				1205	148
57D	88	322	234	2780	2.93	157	1424	1368	56	6090	13.8	93.8	0.60				1190	132
58D	93	248	155	4480	6.27	168	1437	1299	138	4520	7.69	171	1.02				1200	140
59D	94	266	172	3930	5.24	164	1424	1308	116	4490	7.64	143	0.87				1180	139
60D	95	285	190	3260	4.07	150	1415	1299	116	4500	7.60	144	0.96				1165	129
61D	100	326	226	2430	2.75	133	1420	1330	90	4380	7.26	109	0.82				1160	115

TABLE III.— STEWART – WARNER #1 SLOTTED-FIN TYPE HEATER

UC #1 AIR – SHROUD —— CENTRAL CORE NOT IN GAS SIDE

Run No.	AIR SIDE T_{a_1} °F	T_{a_2} °F	ΔT_a °F	W_a lb/hr	$\Delta P'_a$ Inches H_2O	q_a K Btu/hr	EXHAUST – GAS SIDE T_{g_1} °F	T_{g_2} °F	ΔT_g °F	W_g lb/hr	$\Delta P'_g$ Inches H_2O	q_g K Btu/hr	$\frac{q_g}{q_a}$	HEATER TEMPS. t_a °F	t_b °F	t_c °F	OVERALL PERFORMANCE Δt_{lm} °F	(UA) Btu/hr °F
99	90	258	168	4320	5.29	176	1426	1375	51	6860	9.76	96.1	0.55	684	922	598	1220	144
100	90	292	202	3450	3.70	167	1434	1391	43	6880	9.82	81.4	0.49	744	981	650	1215	137
101	94	323	229	2730	2.52	148	1410	1364	46	6870	9.63	87.0	0.59	783	1003	684	1170	126
102	92	363	271	2170	1.65	140	1405	1371	34	6900	9.72	64.5	0.46	825	1053	735	1160	121
103	89	246	157	4320	5.21	164	1403	1339	64	5890	7.30	104	0.63	750	884	563	1205	136
104	90	285	195	3430	3.60	162	1420	1374	46	5920	7.35	74.8	0.46	727	956	624	1205	134
105	91	316	225	2690	2.44	147	1424	1380	44	5910	7.31	71.5	0.49	778	1011	672	1195	123
106	92	359	267	2150	1.65	139	1427	1394	33	5920	7.35	53.6	0.39	825	1057	727	1175	118
107	98	329	231	2140	1.57	120	1390	1329	61	4490	4.13	75.4	0.63	723	1015	650	1145	105
108	94	292	198	2740	2.35	131	1408	1328	80	4500	4.15	99.0	0.76	680	960	594	1175	111
109	94	258	164	3470	3.54	138	1401	1296	105	4500	4.12	130	0.94	628	905	545	1170	118
110	94	230	136	4400	5.14	145	1400	1295	105	4500	4.13	130	0.90	576	855	502	1180	123

TABLE IV.– STEWART – WARNER #1 SLOTTED-FIN TYPE HEATER

UC #1 AIR-SHROUD —— CENTRAL CORE IN GAS SIDE

Run No.	← AIR SIDE → T_{a_1} °F	T_{a_2} °F	ΔT_a °F	W_a lb/hr	$\Delta P_a'$ Inches H_2O	q_a Btu/hr	← EXHAUST-GAS SIDE → T_{g_1} °F	T_{g_2} °F	ΔT_g °F	W_g lb/hr	$\Delta P_g'$ Inches H_2O	q_g Btu/hr	$\frac{q_g}{q_a}$	HEATER TEMPS. t_a °F	t_b °F	t_c °F	OVERALL PERFORMANCE Δt_{lm} °F	(UA) $\frac{Btu}{hr\ °F}$
82D	97	282	185	4250	5.20	190,000	1420	—	—	6800	16.55	—	—	702	958	776	1220	156
83D	97	313	216	3450	3.78	180,000	1420	1373	47	6800	16.66	88,000	.490	748	1007	775	1195	151
84D	100	346	246	2740	2.61	163,000	1424	1377	47	6770	16.65	87,500	.537	796	1046	860	1175	139
85D	100	380	280	2150	1.77	145,000	1424	1390	34	6770	16.82	63,400	.437	896	1085	902	1200	121
86D	99	371	272	2170	1.75	143,000	1415	1360	55	5800	13.40	88,000	.613	754	1064	757	1140	125
87D	96	333	237	2750	2.64	158,000	1424	1368	56	5800	13.46	89,500	.565	772	1028	684	1180	134
88D	95	299	204	3450	3.77	170,000	1407	1338	69	5810	13.45	110,000	.646	714	974	663	1175	145
89D	94	268	174	4250	5.23	179,000	1404	1331	73	5840	13.50	117,000	.655	667	926	622	1180	152
90D	94	255	161	4320	5.16	168,000	1415	1299	116	4490	8.08	143,000	.852	622	897	574	1180	142
91D	96	289	193	3400	3.59	159,000	1424	1321	103	4490	8.05	127,000	.800	676	955	624	1175	135
92D	99	324	225	2740	2.45	149,000	1424	1343	81	4480	7.97	100,000	.670	723	1006	672	1170	127
93D	101	364	263	2130	1.63	136,000	1424	1351	73	4470	8.01	89,700	.660	780	1055	727	1150	118

TABLE V.– STEWART – WARNER #1 SLOTTED-FIN TYPE HEATER

UC #2 AIR – SHROUD ——— CENTRAL CORE NOT IN GAS SIDE

	AIR SIDE						EXHAUST – GAS SIDE							HEATER TEMPS.			OVERALL PERFORMANCE	
Run No.	T_{a_1} °F	T_{a_2} °F	ΔT_a °F	W_a lb/hr	$\Delta P'_a$ Inches H_2O	q_a KBtu/hr	T_{g_1} °F	T_{g_2} °F	ΔT_g °F	W_g lb/hr	$\Delta P'_g$ Inches H_2O	q_g KBtu/hr	$\frac{q_g}{q_a}$	t_a °F	t_b °F	t_c °F	Δt_{lm} °F	(UA) Btu/hr °F
111	90	242	152	4280	3.06	158	1411	1360	51	6920	9.83	96.9	0.61	688	962	663	1220	129
112	91	271	180	3420	2.14	149	1405	1369	36	6900	9.87	68.2	0.46	763	1020	714	1200	124
113	89	298	209	2670	1.40	135	1409	1372	37	6920	9.75	70.4	0.52	790	1063	763	1195	113
114	92	329	237	2140	0.96	123	1402	1364	38	6900	9.80	72.0	0.59	842	1106	823	1180	104
115	93	319	226	2120	1.00	116	1398	1361	37	5850	7.02	59.5	0.51	808	1074	788	1180	98
116	93	288	195	2740	1.40	129	1392	1352	40	5850	7.02	63.2	0.49	759	1028	733	1200	107
117	92	259	167	3470	2.15	140	1393	1340	53	5850	7.02	85.2	0.61	701	977	672	1190	118
118	90	226	136	4590	3.25	151	1384	1330	54	5850	7.00	86.8	0.58	643	920	609	1200	126
119	91	221	130	4600	3.28	145	1416	1344	72	4500	4.31	87.1	0.60	611	901	581	1220	119
120	90	248	158	3590	2.20	137	1422	1358	64	4510	4.37	79.4	0.58	665	970	639	1215	113
121	93	280	187	2780	1.45	126	1430	1374	56	4500	4.31	68.5	0.54	721	1020	701	1215	104
122	95	314	219	2150	0.90	114	1429	1381	48	4390	4.32	57.9	0.51	778	1078	766	1200	95

TABLE VI.– STEWART - WARNER #1 SLOTTED-FIN TYPE HEATER

UC #2 AIR – SHROUD —— CENTRAL CORE IN GAS SIDE

	AIR SIDE						EXHAUST – GAS SIDE							HEATER TEMPS.			OVERALL PERFORMANCE	
Run No.	T_{a_1} °F	T_{a_2} °F	ΔT_a °F	W_a lbs/hr	$\Delta P'_a$ Inches H_2O	q_a KBtu/hr	T_{g_1} °F	T_{g_2} °F	ΔT_g °F	W_g lbs/hr	$\Delta P'_g$ Inches H_2O	q_g KBtu/hr	$\frac{q_g}{q_a}$	t_a °F	t_b °F	t_c °F	Δt_{lm} °F	(UA) Btu/hr °F
70D	93	261	168	4190	3.85	170	1413	1374	39	6820	17.0	73.1	0.43	765	1017	724	1210	140
71D	92	270	178	3900	3.50	168	1412	1372	40	6840	17.5	75.8	0.45	782	1024	736	1210	139
72D	94	292	198	3250	2.58	156	1420	1368	52	6820	17.4	97.5	0.62	822	1062	782	1200	130
73D	95	334	239	2420	1.58	140	1420	1390	30	6810	17.5	56.2	0.40	891	1122	852	1190	118
74D	83	251	168	4230	3.80	172	1424	1343	81	5810	13.1	129	0.75	718	986	699	1220	141
75D	91	262	171	3940	3.45	163	1435	1351	84	5810	13.1	134	0.82	736	1001	708	1220	134
76D	95	285	190	3200	2.45	147	1420	1356	64	5800	13.1	102	0.69	786	1044	740	1195	123
77D	93	323	230	2450	1.60	136	1428	1360	60	5830	13.1	96.2	0.71	848	1094	822	1180	115
78D	93	238	145	4330	3.80	152	1415	1326	89	4430	7.95	108	0.71	690	955	674	1205	126
79D	95	246	151	3980	3.36	146	1412	1319	93	4280	7.29	110	0.75	699	955	690	1200	122
80D	93	271	178	3300	2.46	142	1459	1335	124	4290	7.33	146	1.03	735	978	729	1210	117
81D	96	304	208	2520	1.66	127	1420	1350	70	4310	7.31	83.0	0.65	751	1122	808	1185	107

TABLE VII

STEWART-WARNER SLOTTED-FIN HEATER

Isothermal Pressure Drop Data[a]
Ventilating-Air Side

W_a lb/hr	G_a lb/ft^{2}hr	ΔP_{DUCT} lb/ft^2	ΔP_{HTR} lb/ft^2	$\Delta P_{T_{iso}}$ lb/ft^2	$\left(\zeta_{iso} \cdot \frac{L}{D_a}\right)$
1. Using Ames Air Shroud					
2000	7,380	2.60	6.50	9.10	7.03
3000	11,100	6.40	12.4	18.8	5.84
4000	14,800	10.2	21.3	31.5	5.78
5000	18,400	19.8	27.2	47.0	4.71
2. Using UC-1 Air Shroud					
2000	9,860	0.73	4.02	4.75	2.45
3000	14,800	1.55	8.4	10.0	2.28
4000	19,700	2.70	14.8	17.5	2.27
5000	24,600	4.15	22.6	26.8	2.20
3. Using UC-2 Air Shroud					
2000	7,380	0.73	2.52	3.25	2.73
3000	11,100	1.55	5.45	7.00	2.63
4000	14,800	2.70	9.5	12.2	2.53
5000	18,400	4.15	14.6	18.8	2.54

[a] Pressure drops obtained from plots of ΔP versus W_a

ΔP_{DUCT} = Pressure drop in air shroud ducts (entrance and exit sections), lb/ft^2

ΔP_{HTR} = Pressure drop in heater, lb/ft^2

$\Delta P_{T_{iso}}$ = Overall pressure drop = $\Delta P_{DUCT} + \Delta P_{HTR}$, lb/ft^2

$$\left(\zeta_{iso} \cdot \frac{L}{D_a}\right) = 2 \cdot g \cdot \gamma \, \frac{\Delta P_{HTR}}{\left(\frac{G_a}{3600}\right)^2} \tag{10a}$$

TABLE VIII

STEWART-WARNER SLOTTED-FIN HEATER

Isothermal Pressure Drop Data[b]
Exhaust-Gas Side

W_g lb/hr	G_g lb/ft^2 hr	$\Delta P_{T_{iso}} = \Delta P_{HTR}$ lb/ft^2	$\left(\zeta_{iso} \cdot \frac{L}{D_g}\right)$
1. Without Central Core			
4000	19,700	4.60	0.699
6000	29,500	9.70	0.658
10000	49,200	25.0	0.610
2. With Central Core			
4000	23,200	9.40	1.03
6000	34,800	19.9	0.956
10000	58,100	51.3	0.889

[b] Pressure drops obtained from plots of ΔP versus W_g

$\Delta P_{T_{iso}}$ = Overall pressure drop, lb/ft^2

ΔP_{HTR} = Pressure drop across heater only, lb/ft^2

$$\left(\zeta_{iso} \cdot \frac{L}{D_g}\right) = 2 \cdot g \cdot \gamma \, \frac{\Delta P_{HTR}}{\left(\frac{G_g}{3600}\right)^2} \tag{10}$$

TABLE IX

STEWART-WARNER SLOTTED-FIN HEATER

Non-Isothermal Pressure Drop Data
Ventilating-Air Side

Run No.	W_a lb /hr	G_a lb/hr ft^2	Measured isothermal pressure drop(c) $\Delta P_{T_{iso}}$ lb /ft^2	Predicted non-isothermal pressure drop ΔP lb/ft^2	Measured non-isothermal pressure drop ΔP lb /ft^2	T_1 ^oR	T_2 ^oR	T_a ^oR
1. Ames Air Shroud			T_{iso} 558^oR					
31	2600	10,700	14.0	18.8	23.3	557	782	669
40	3460	14,200	23.5	29.9	37.4	564	742	653
24	4190	17,200	33.5	40.7	50.5	555	699	627
38	4980	20,500	45.5	56.0	74.5	564	714	639
46	5580	22,900	56.0	67.9	82.0	550	683	616
2. UC-2 Air Shroud			T_{iso} 552^oR					
77D	2450	8,800	4.80	7.00	8.30	553	783	668
76D	3200	11,600	7.90	11.2	12.7	555	745	650
75D	3940	14,300	11.8	15.9	17.9	551	722	636
74D	4230	15,300	13.7	18.5	19.7	553	711	632
3. UC-1 Air Shroud			T_{iso} 551^oR					
85D	2150	10,300	5.45	8.73	8.90	560	840	700
84D	2740	13,100	8.60	13.3	13.4	560	806	683
83D	3450	16,500	13.3	19.7	19.5	557	773	670
82D	4250	20,300	19.7	27.9	27.3	557	742	650

(c) Obtained from plot of $\Delta P_{T_{iso}}$ versus W_a

$$\Delta P = \Delta P_{T_{iso}} \left(\frac{T_a}{T_{iso}}\right)^{1.13} + \left(\frac{G_a}{3600}\right)^2 \frac{1}{\gamma_1 \cdot g}\left(\frac{T_2}{T_1} - 1\right) \quad (11)$$

TABLE X

STEWART-WARNER SLOTTED-FIN HEATER

Non-Isothermal Pressure Drop Data
Exhaust-Gas Side

Run No.	W_g lbs/hr	G_g lbs/hrft^2	Measured isothermal pressure drop(d) $\Delta P_{T_{iso}}$ lbs/ft^2	Predicted non-isothermal pressure drop ΔP lbs/ft^2	Measured non-isothermal pressure drop ΔP lbs/ft^2	T_1 ^oR	T_2 ^oR	T_a ^oR
1. Without Central Core			T_{iso} 561^oR					
24	4280	20,500	5.20	17.2	16.3	1880	1772	1826
28	5970	27,500	9.60	33.0	32.4	1915	1816	1865
35	7020	33,600	13.0	44.6	45.1	1867	1803	1835
39	7530	36,000	14.7	47.1	49.3	1850	1755	1802
2. With Central Core			T_{iso} 551^oR					
61D	4380	24,600	11.0	39.3	37.7	1880	1790	1835
60D	4500	25,300	11.7	40.3	39.4	1875	1759	1817
55D	6160	34,600	21.0	75.4	71.6	1884	1794	1839
48D	6880	38,700	25.1	89.6	83.1	1897	1790	1843

(d) Obtained from plot of $\Delta P_{T_{iso}}$ versus W_g.

$$\Delta P = \Delta P_{T_{iso}} \left(\frac{T_a}{T_{iso}}\right)^{1.13} + \left(\frac{G}{3600}\right)^2 \frac{1}{\gamma_1 \cdot g}\left(\frac{T_2}{T_1} - 1\right) \quad (11)$$

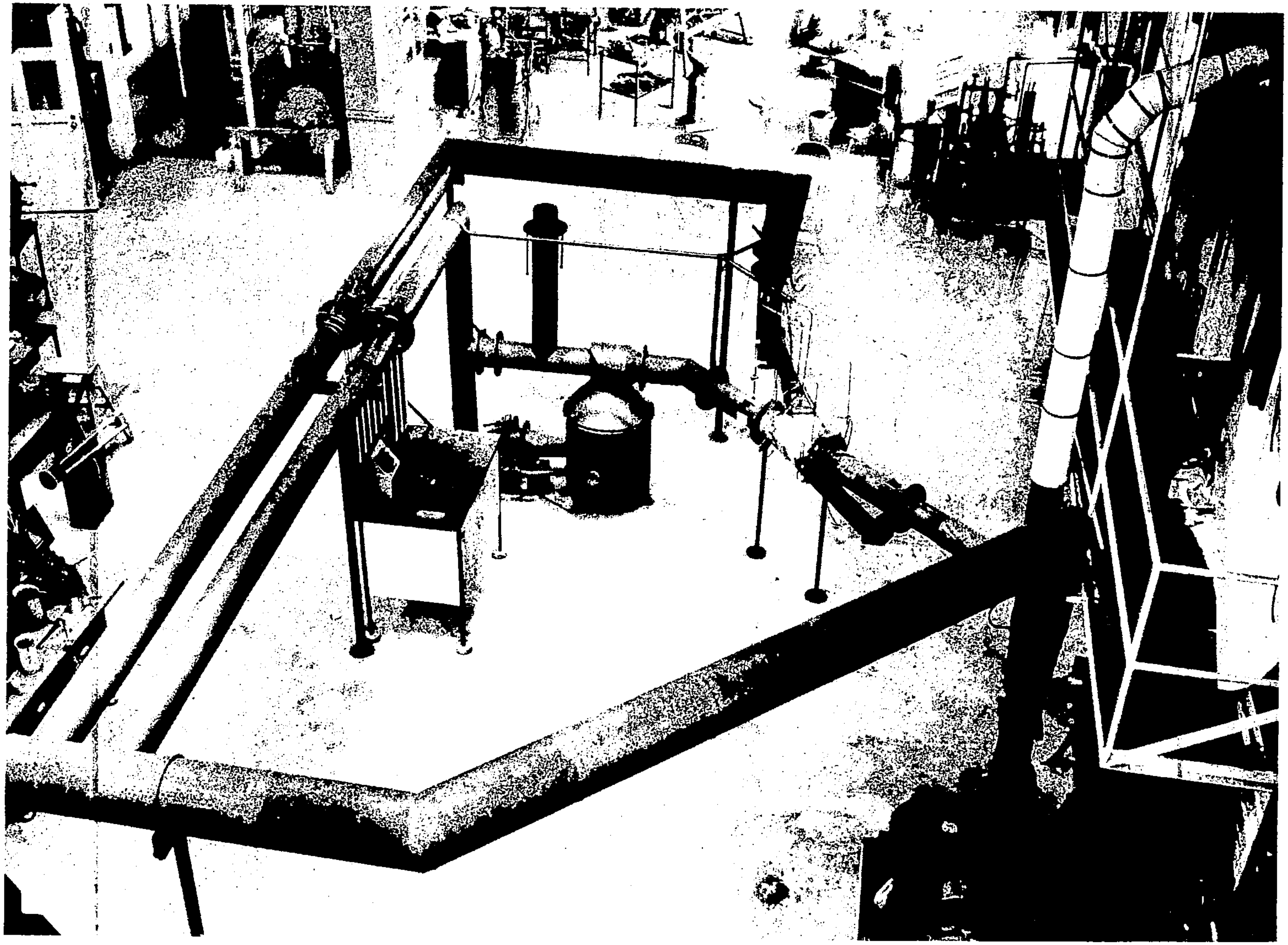

Figure 1.- Photograph of heater test stand.

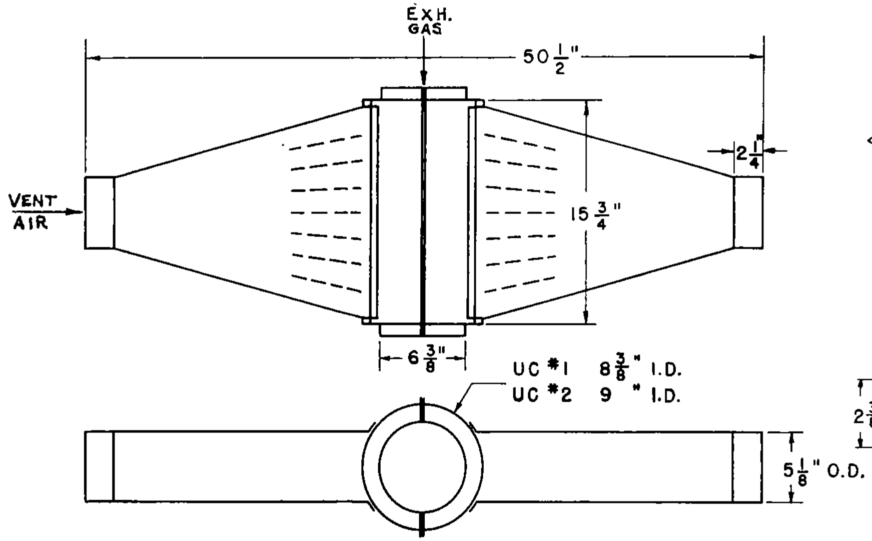

UC #1 and UC #2 air shrouds

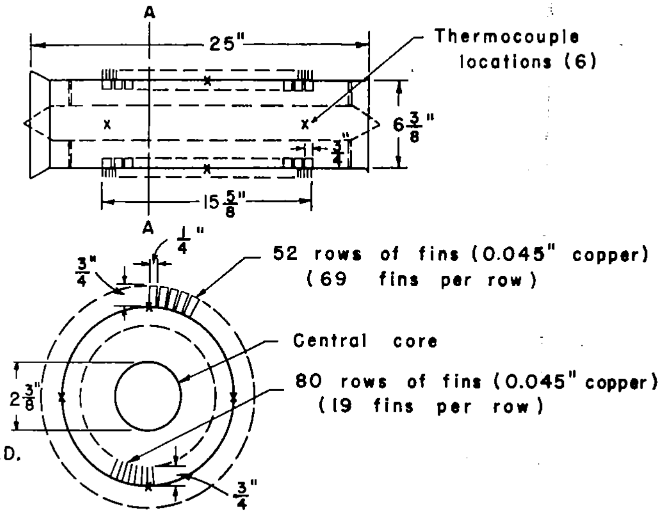

Section – A-A

Stewart-Warner slotted-fin heater with central core

wt. – 32.5 lbs (without core)

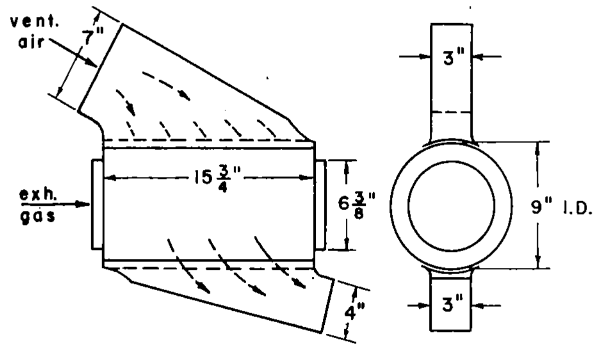

Ames air shroud
wt. – 6.0 lbs

	Air side			Gas side	
	UC#1	UC#2	Ames	without core	with core
Cross-sect. area, ft^2	0.203	0.271	0.271	0.203	0.172
Total wetted perim., ft	18.6	18.7	18.7	11.7	12.3
Hydraulic diameter, ft	0.0436	0.0580	0.0580	0.0694	0.0559

Fig. 2. - Schematic Diagram of Stewart-Warner Slotted-Fin Heater with Central Core and Ames and UC Air Shrouds.

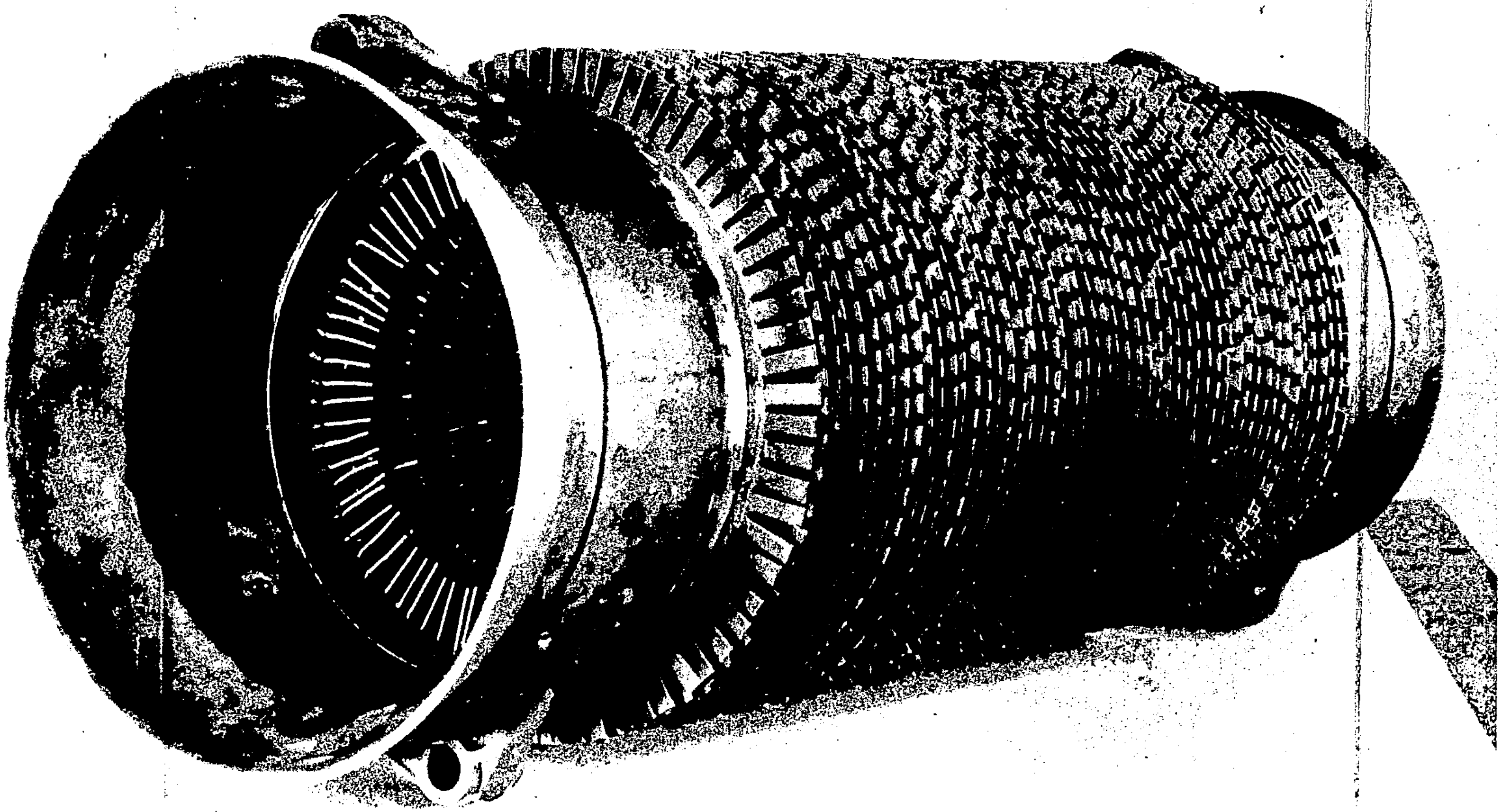

Figure 3.- Photograph of Stewart-Warner slotted-fin heater.

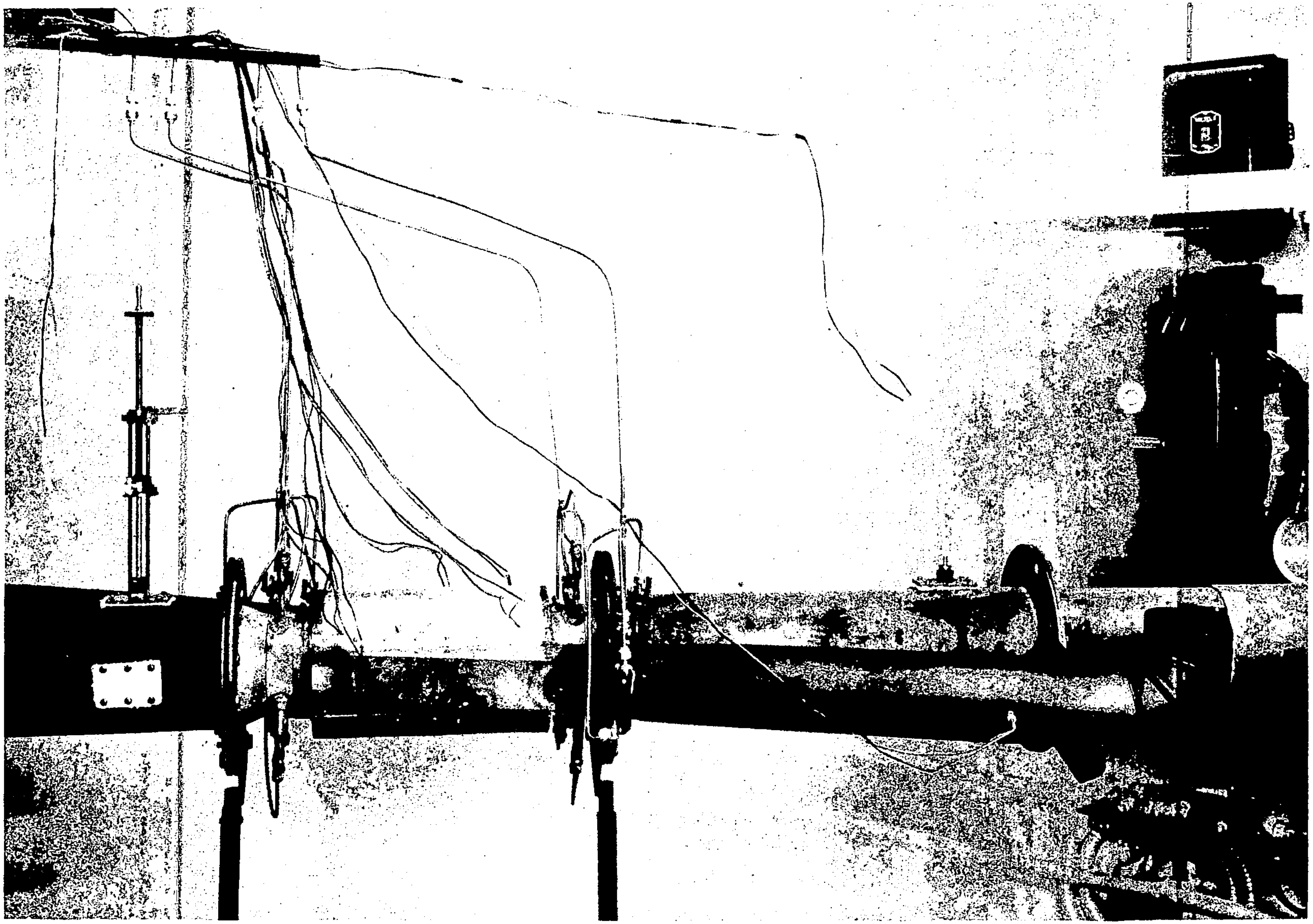

Figure 4.- Photograph of Stewart-Warner heater using semi-cross-flow (Ames) air shroud. (Taken before installation of traversing, shielded thermocouple at exhaust-gas outlet.)

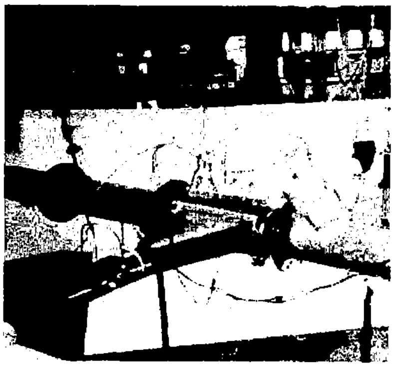

Figure 5.- Photograph of Stewart-Warner heater using UC-1 or UC-2 air shroud.

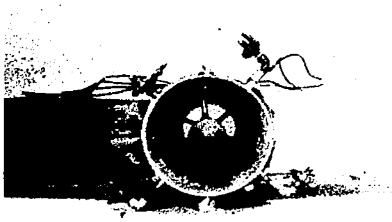

Figure 6.- Photograph showing central core installed in exhaust-gas side of Stewart-Warner heater.

(1 block = 10 divisions on 1/20 Engr. scale)

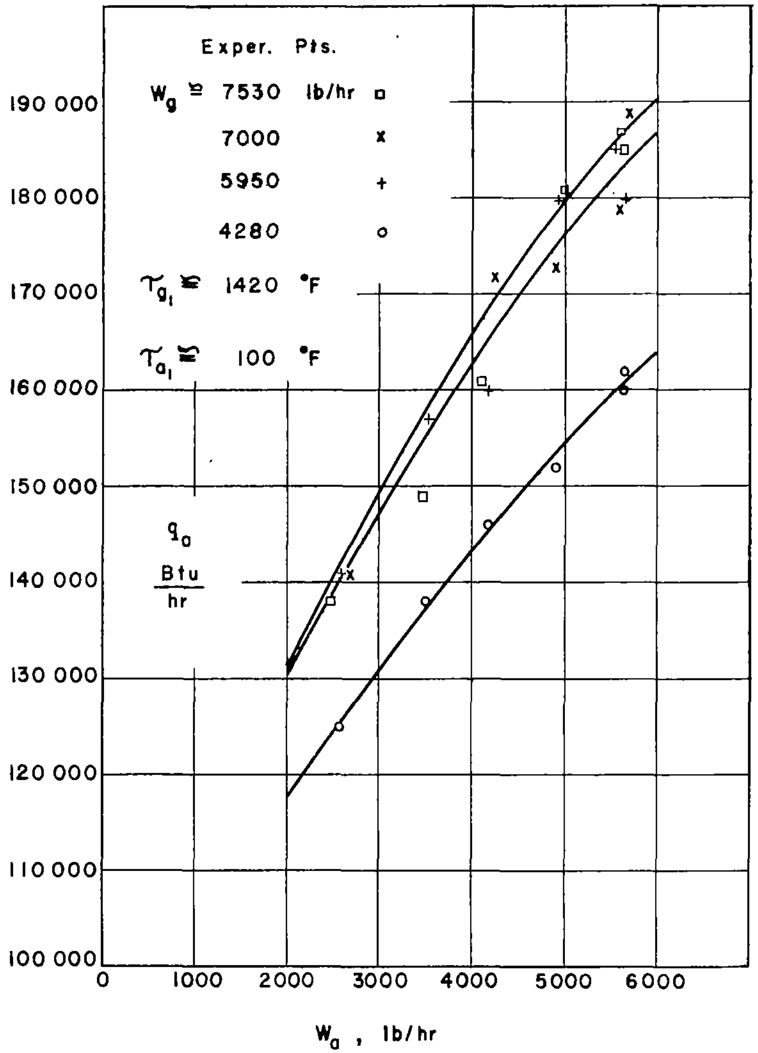

Fig. 7.- Thermal output of Stewart-Warner heater without central core, using Ames air shroud, as a function of ventilating-air rate.

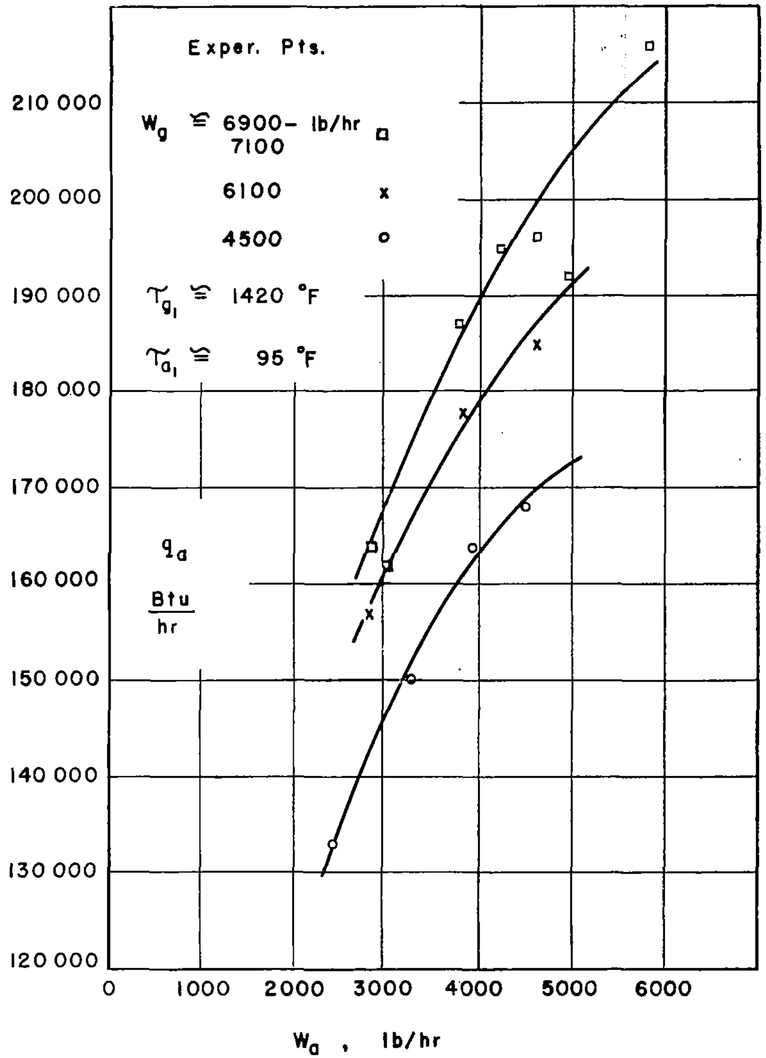

Fig. 8.- Thermal output of Stewart-Warner heater with central core, using Ames air shroud, as a function of ventilating-air rate.

NACA

Figs. 7,8

(1 block = 10/20")

NACA

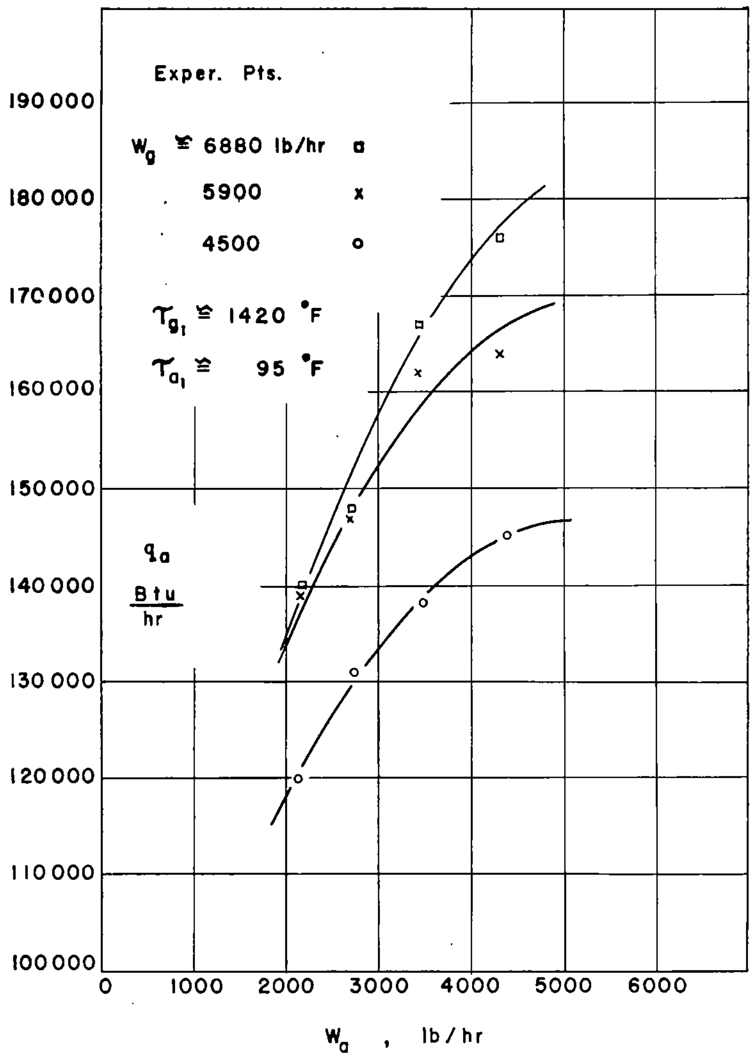

Fig. 9.- Thermal output of Stewart-Warner heater without central core, using UC #1 air shroud, as a function of ventilating-air rate.

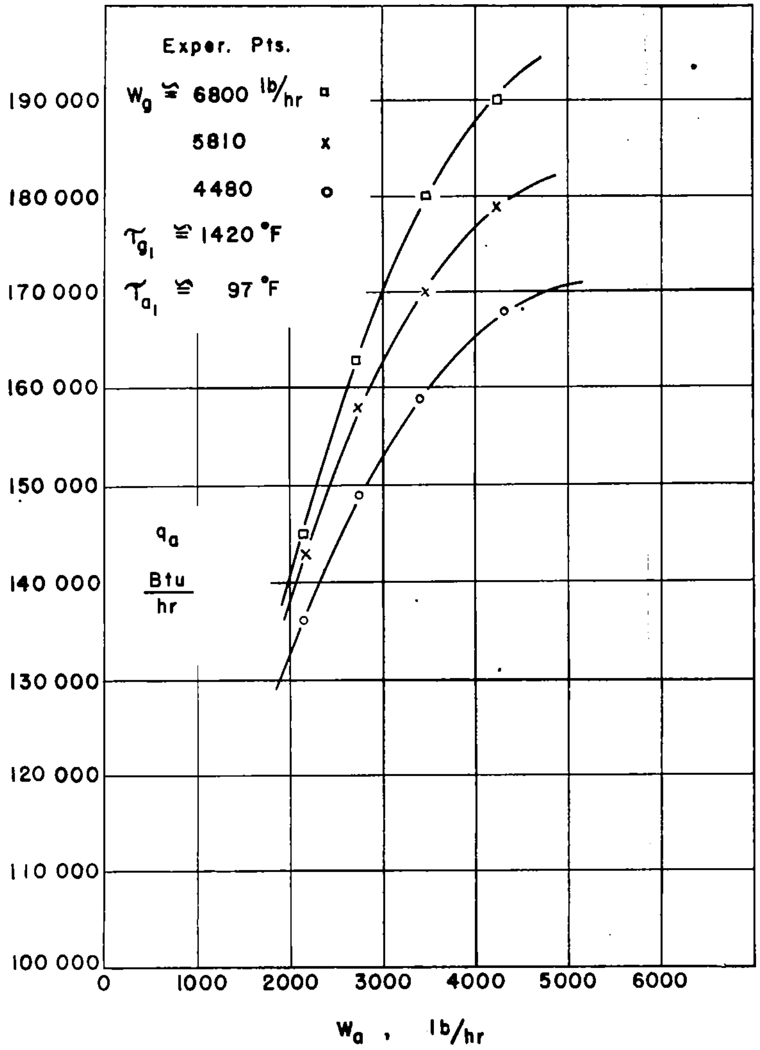

Fig. 10.- Thermal output of Stewart-Warner heater with central core, using UC #1 air shroud, as a function of ventilating-air rate.

Figs. 9,10

(1 block = 10/20")

NACA

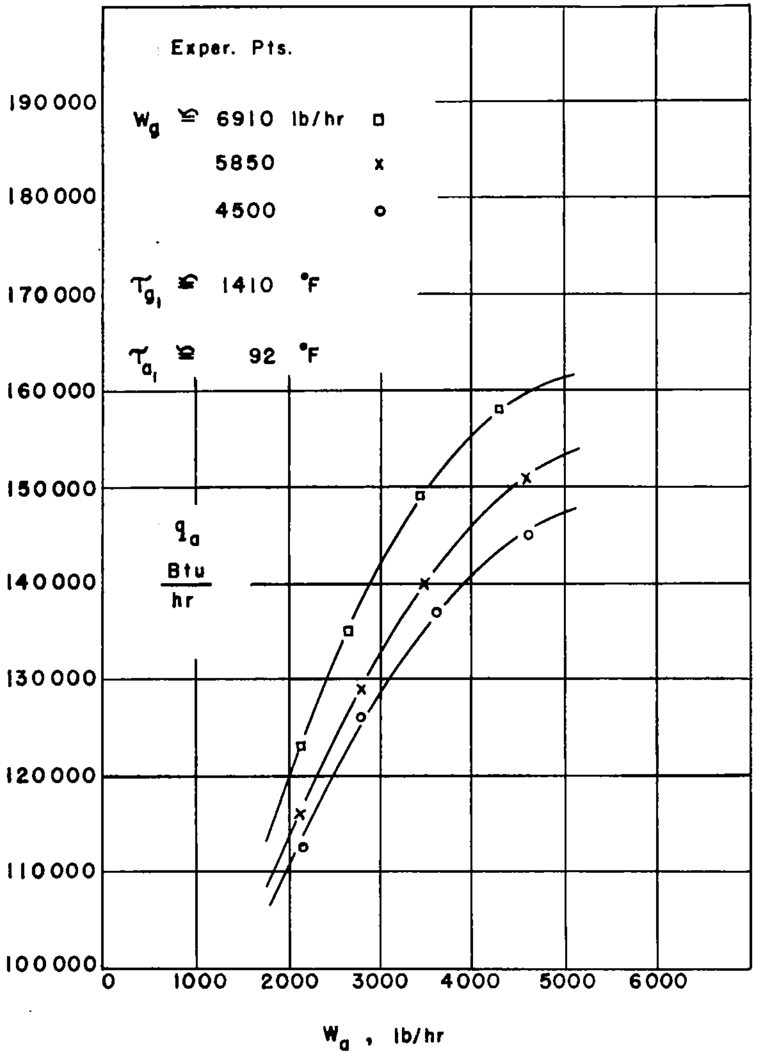

Fig. 11.- Thermal output of Stewart-Warner heater without central core, using UC #2 air shroud, as a function of ventilating-air rate.

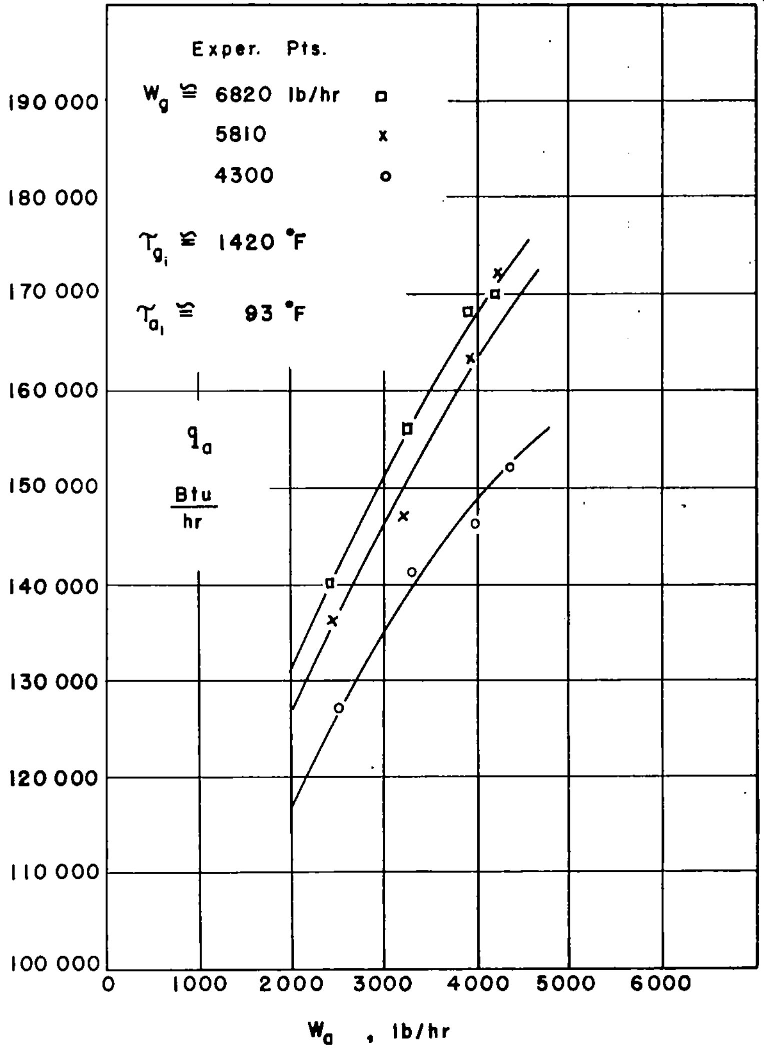

Fig. 12.- Thermal output of Stewart-Warner heater with central core, using UC #2 air shroud, as a function of ventilating-air rate.

Figs. 11,12

(1 block = 10/20")

NACA

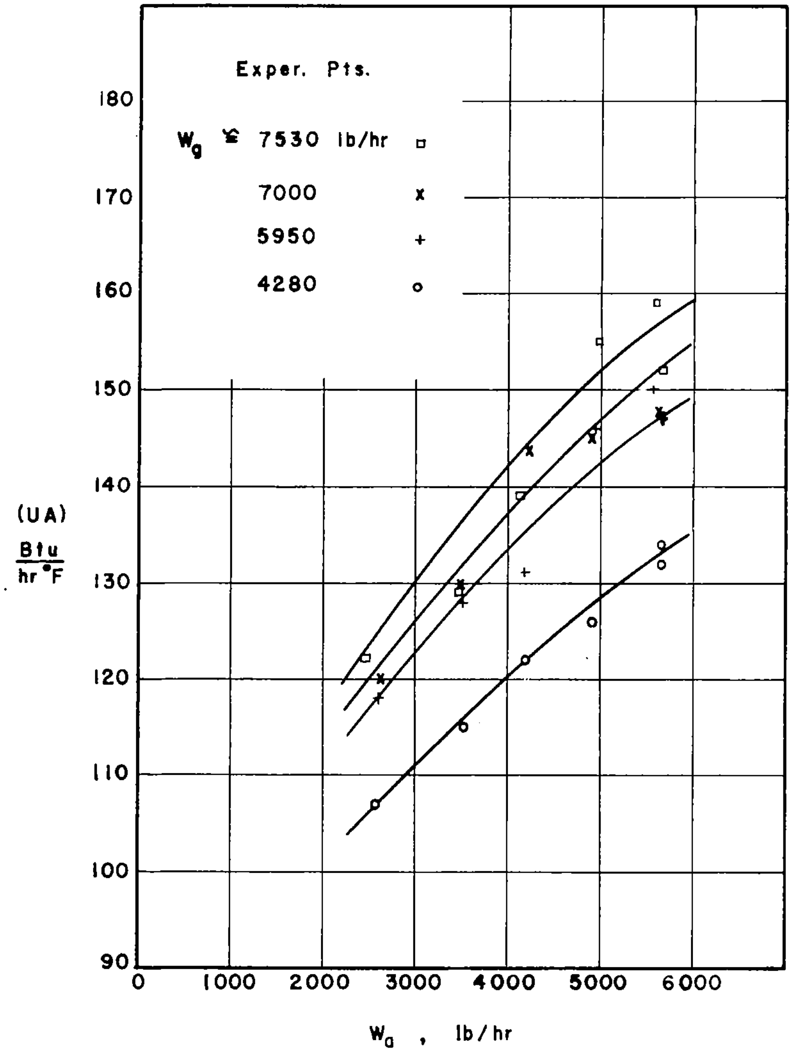

Fig. 13.- Overall thermal conductance of Stewart - Warner heater without central core, using Ames air shroud, as a function of ventilating - air rate.

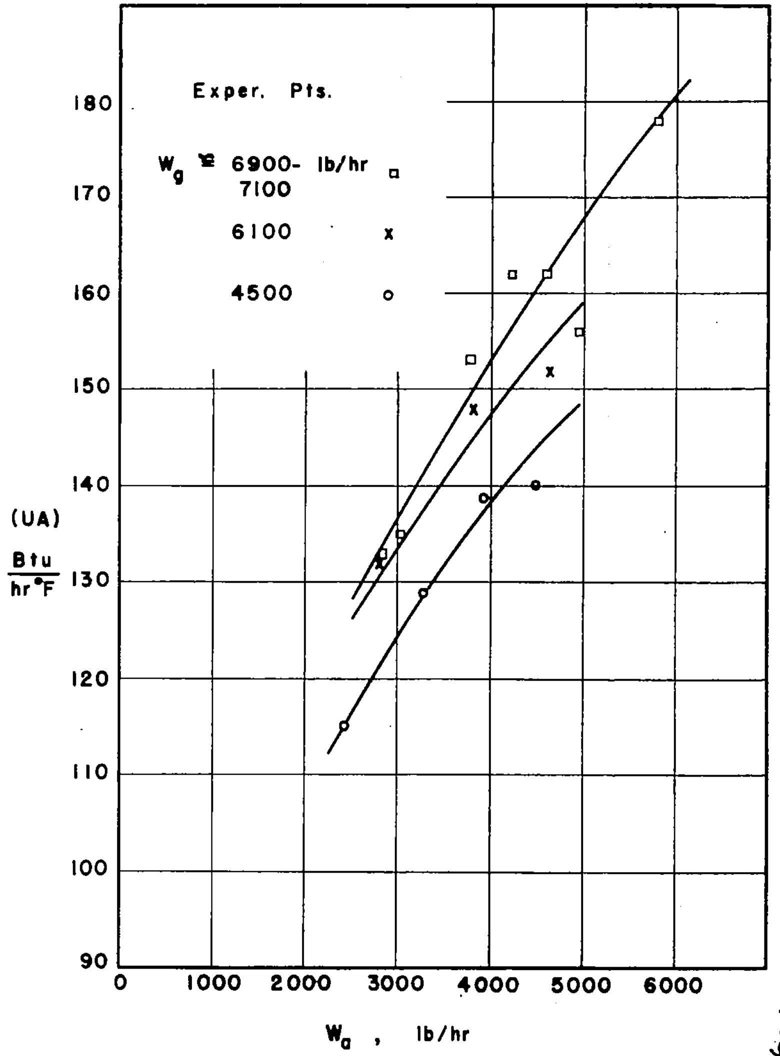

Fig. 14.- Overall thermal conductance of Stewart - Warner heater with central core, using Ames air shroud, as a function of ventilating - air rate.

Figs. 13,14

(1 block = 10/20")

NACA

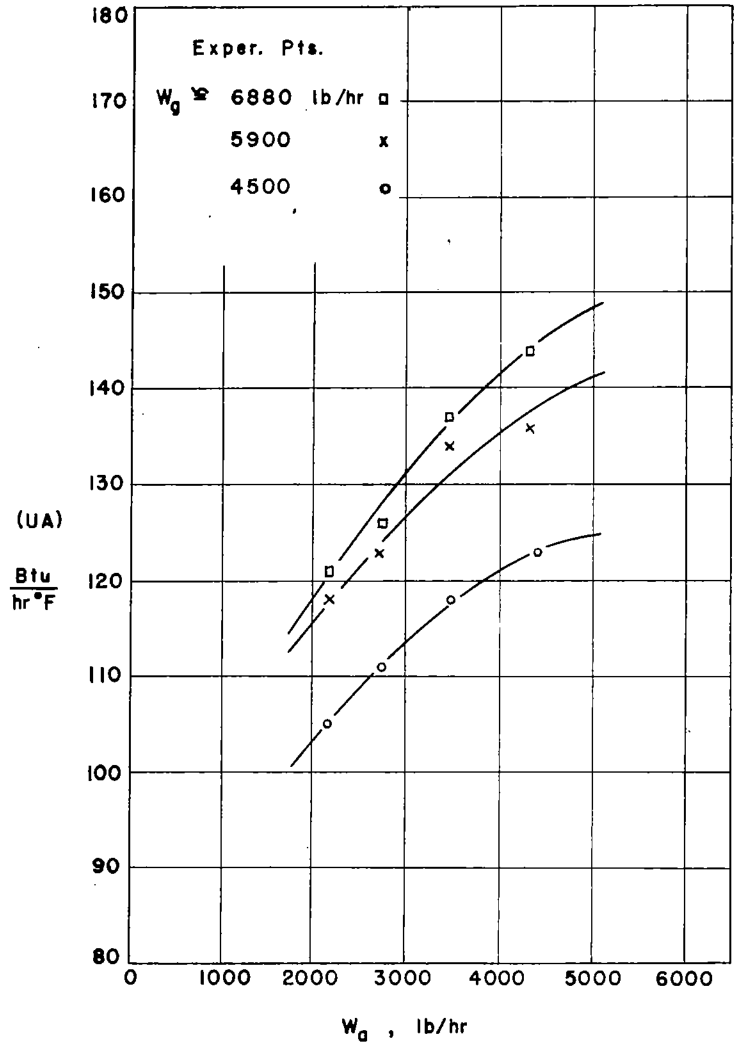

Fig. 15.- Overall conductance of Stewart - Warner heater without central core, using UC #1 air shroud, as a function of ventilating - air rate.

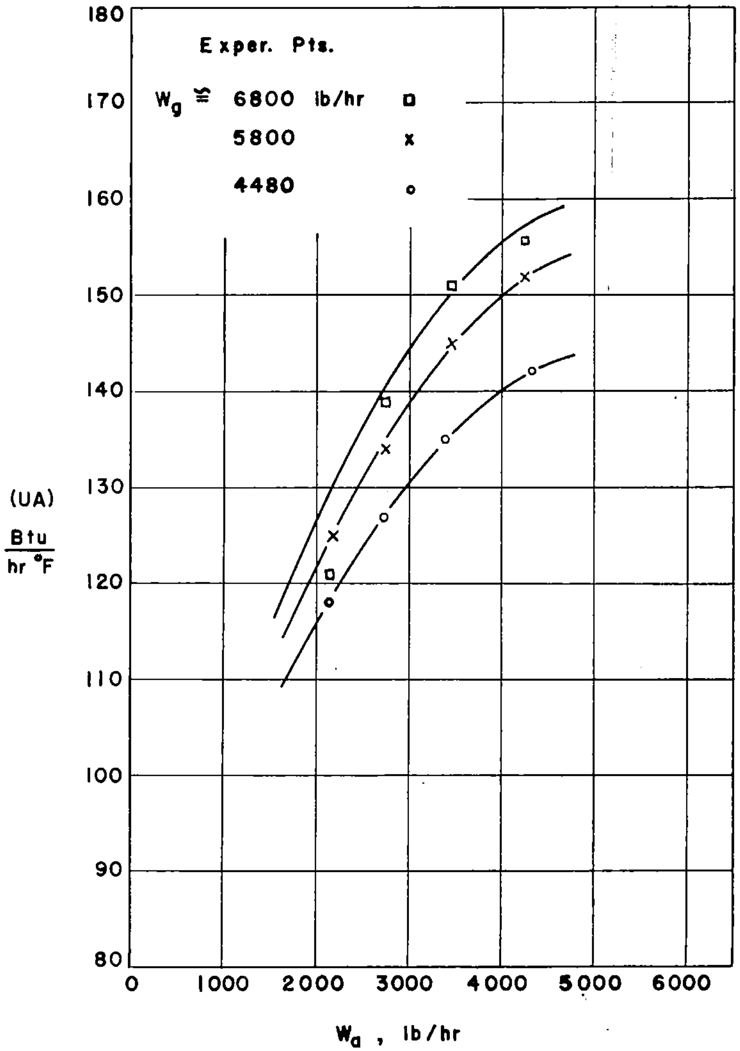

Fig. 16.- Overall conductance of Stewart - Warner heater with central core, using UC #1 air shroud, as a function of ventilating - air rate.

Figs. 15,16

(1 block = 10/20")

NACA

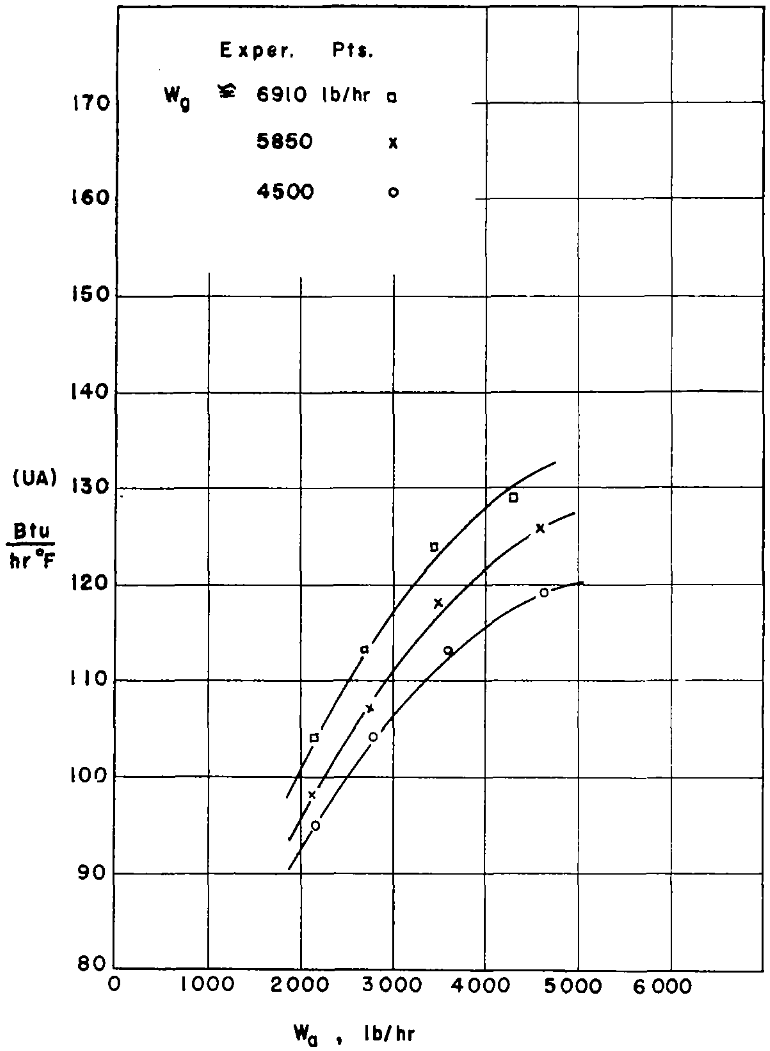

Fig. 17.- Overall thermal conductance of Stewart-Warner heater without central core, using UC #2 air shroud, as a function of ventilating-air rate.

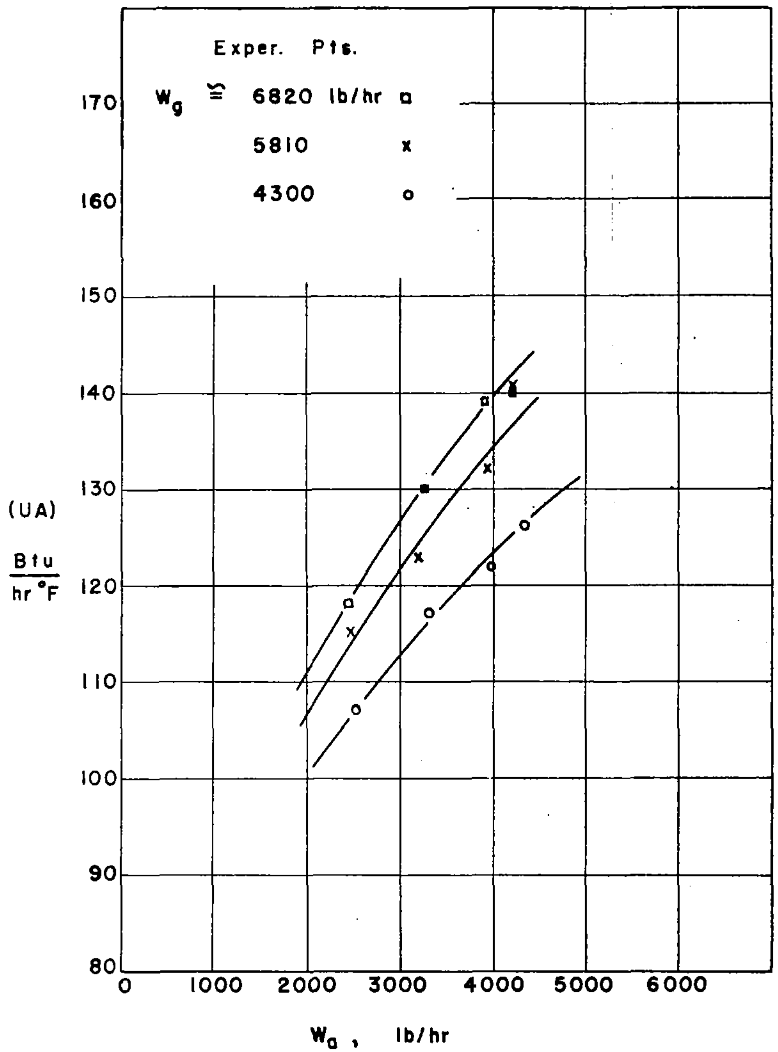

Fig. 18.- Overall thermal conductance of Stewart - Warner heater with central core, using UC #2 air shroud, as a function of ventilating - air rate.

Figs. 17,18

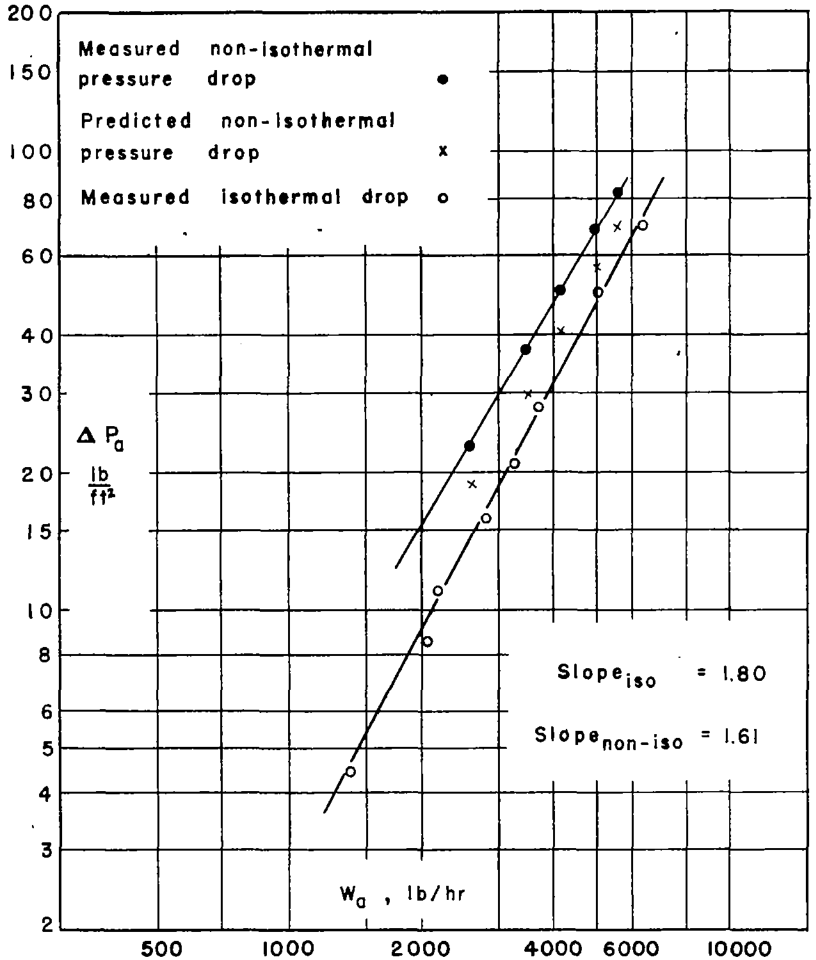

Fig. 19.- Pressure drop on air side of Stewart-Warner heater with Ames air shroud, as a function of ventilating-air rate

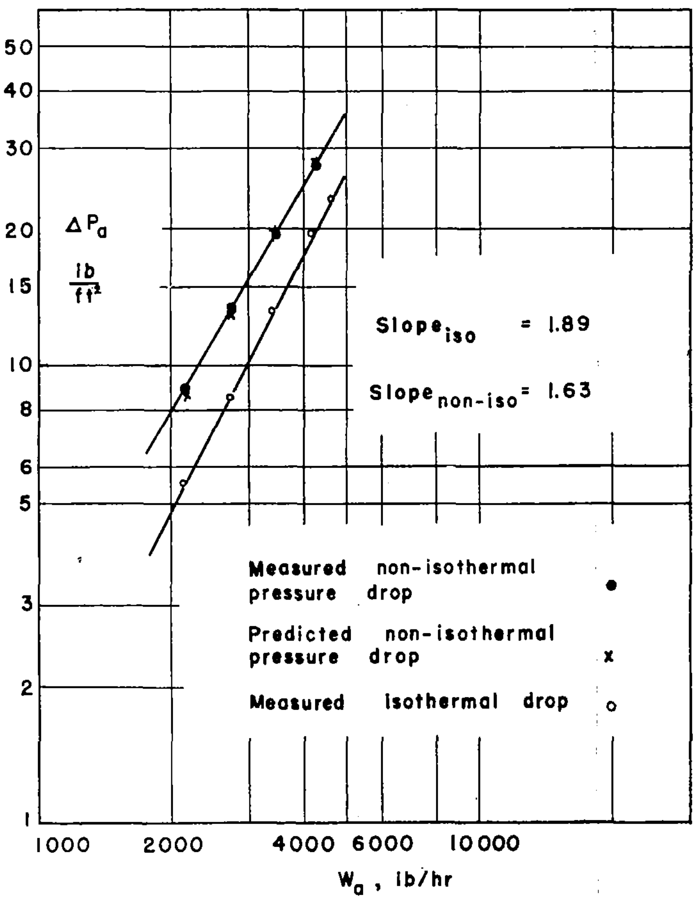

Fig. 20.- Pressure drop on air side of Stewart - Warner heater with UC #1 air shroud, as a function of ventilating - air rate.

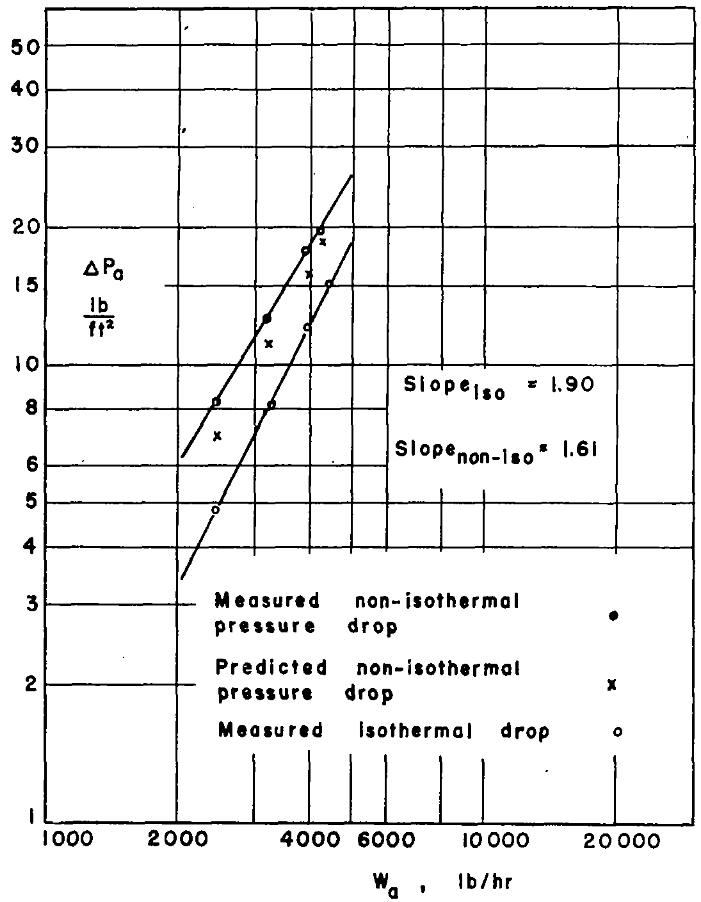

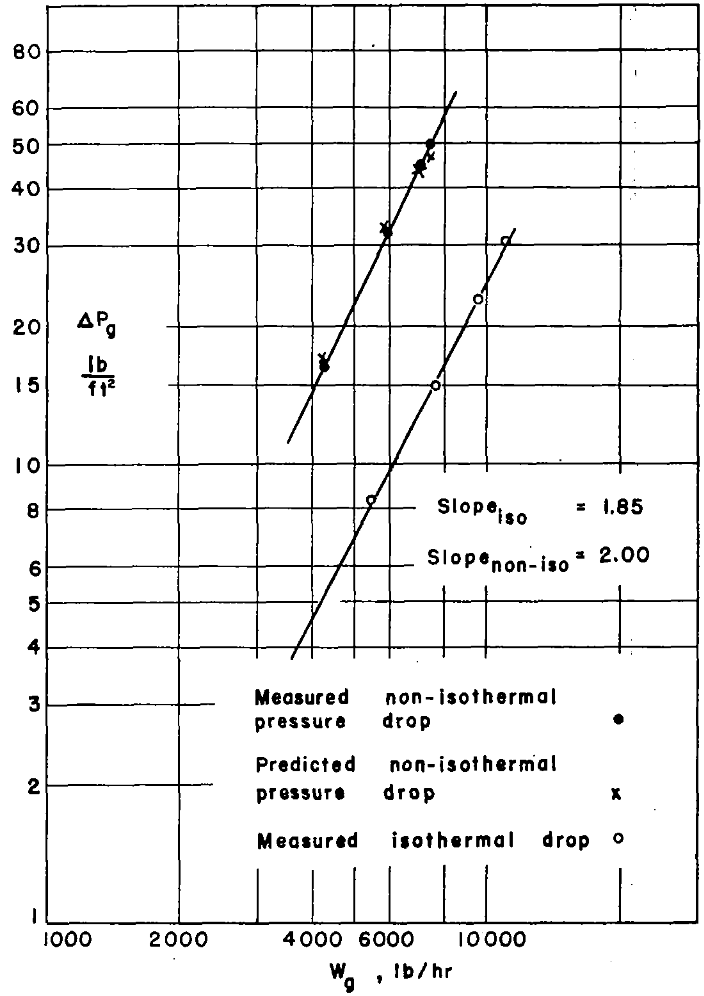

Fig. 21.- Pressure drop on air side of Stewart - Warner heater, with UC #2 air shroud, as a function of ventilating - air rate.

Fig. 22.- Pressure drop on exhaust - gas side of Stewart-Warner heater, without central core, as a function of exhaust - gas rate.

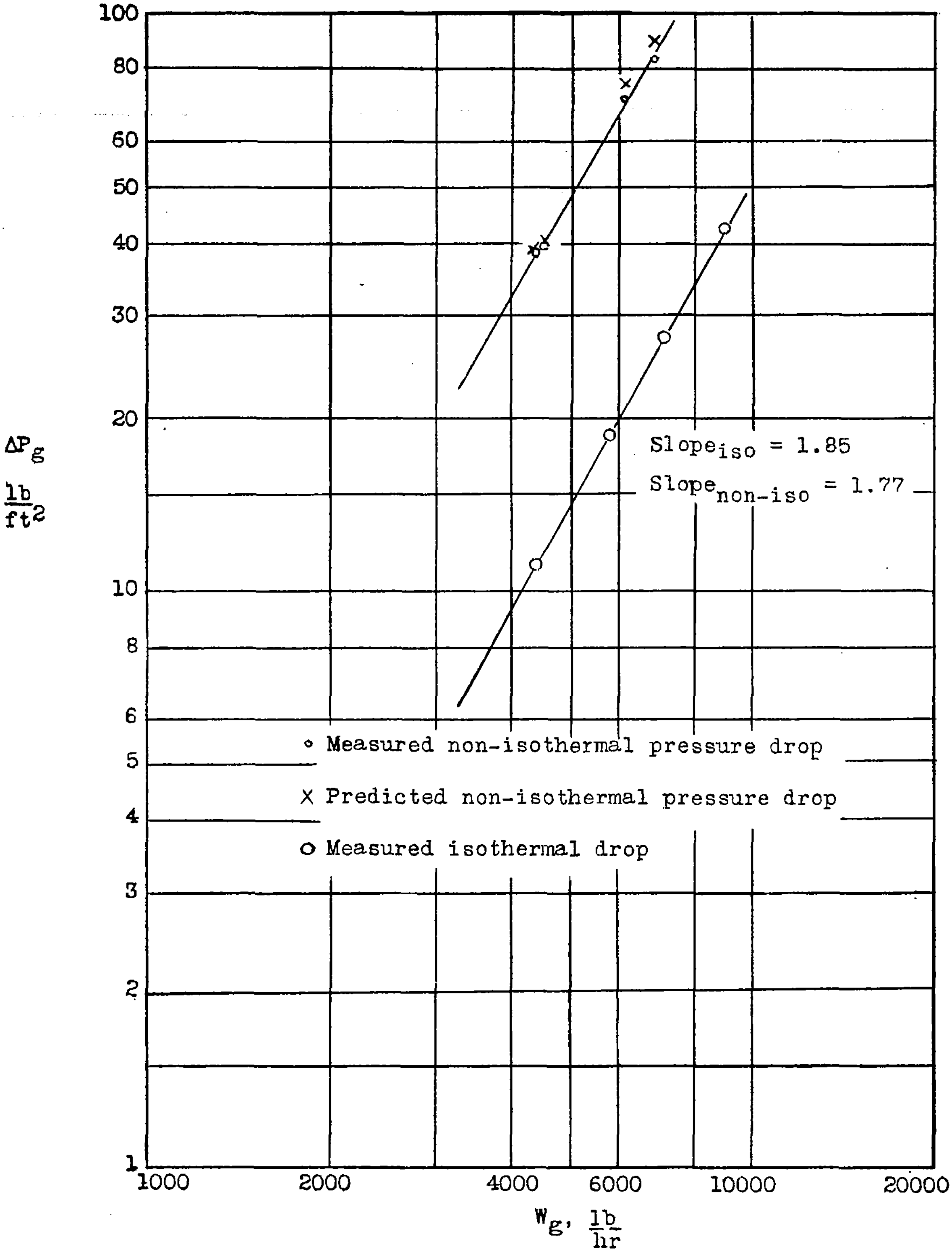

Figure 23.- Pressure drop on exhaust-gas side of Stewart-Warner heater, with central core, as a function of exhaust-gas rate.